



Calhoun: The NPS Institutional Archive
DSpace Repository

Theses and Dissertations

Thesis and Dissertation Collection

1976

Pulse height analyzer interfacing and
computer programming in the environmental
laser propagation project.

Plett, John Robert

Monterey, California. Naval Postgraduate School

<http://hdl.handle.net/10945/17917>

Downloaded from NPS Archive: Calhoun



Calhoun is a project of the Dudley Knox Library at NPS, furthering the precepts and goals of open government and government transparency. All information contained herein has been approved for release by the NPS Public Affairs Officer.

Dudley Knox Library / Naval Postgraduate School
411 Dyer Road / 1 University Circle
Monterey, California USA 93943

<http://www.nps.edu/library>

PULSE HEIGHT ANALYZER INTERFACING AND
COMPUTER PROGRAMMING IN THE
ENVIRONMENTAL LASER PROPAGATION PROJECT

John Robert Plett

NAVAL POSTGRADUATE SCHOOL

Monterey, California



THESIS

PULSE HEIGHT ANALYZER INTERFACING AND
COMPUTER PROGRAMMING IN THE
ENVIRONMENTAL LASER PROPAGATION PROJECT

by

John Robert Plett

June 1976

Thesis Advisor:

E.A. Milne

Approved for public release; distribution unlimited.

T174985

REPORT DOCUMENTATION PAGE		READ INSTRUCTIONS BEFORE COMPLETING FORM
1. REPORT NUMBER	2. GOVT ACCESSION NO.	3. RECIPIENT'S CATALOG NUMBER
4. TITLE (and Subtitle) Pulse Height Analyzer Interfacing and Computer Programming in the Environmental Laser Propagation Project		5. TYPE OF REPORT & PERIOD COVERED Master's Thesis; June 1976
7. AUTHOR(s) John Robert Plett		6. PERFORMING ORG. REPORT NUMBER
9. PERFORMING ORGANIZATION NAME AND ADDRESS Naval Postgraduate School Monterey, California 93940		8. CONTRACT OR GRANT NUMBER(s)
11. CONTROLLING OFFICE NAME AND ADDRESS Naval Postgraduate School Monterey, California 93940		10. PROGRAM ELEMENT, PROJECT, TASK AREA & WORK UNIT NUMBERS
14. MONITORING AGENCY NAME & ADDRESS (if different from Controlling Office)		12. REPORT DATE June 1976
		13. NUMBER OF PAGES 73
		15. SECURITY CLASS. (of this report) Unclassified
		15a. DECLASSIFICATION/DOWNGRADING SCHEDULE
16. DISTRIBUTION STATEMENT (of this Report) Approved for public release; distribution unlimited.		
17. DISTRIBUTION STATEMENT (of the abstract entered in Block 20, if different from Report)		
18. SUPPLEMENTARY NOTES		
19. KEY WORDS (Continue on reverse side if necessary and identify by block number) Pulse Height Analyzer Laser Propagation Interfacing		
20. ABSTRACT (Continue on reverse side if necessary and identify by block number) An effective data interface between a Victoreen PIP-400 pulse-height analyzer and a Hewlett-Packard 9810A calculator was designed, built, and tested. A calculator program was written which enabled a research group studying laser		

(20. ABSTRACT Continued)

propagation in the marine boundary layer to conduct rapid, local processing of scintillation and extinction data.

Pulse Height Analyzer Interfacing and
Computer Programming in the
Environmental Laser Propagation Project

by

John Robert Plett
Lieutenant, United States Navy
B.S., United States Naval Academy, 1969

Submitted in partial fulfillment of the
requirements for the degree of

MASTER OF SCIENCE IN PHYSICS

from the

NAVAL POSTGRADUATE SCHOOL
June 1976

ABSTRACT

An effective data interface between a Victoreen PIP-400 pulse-height analyzer and a Hewlett-Packard 9810A calculator was designed, built, and tested. A calculator program was written which enabled a research group studying laser propagation in the marine boundary layer to conduct rapid, local processing of scintillation and extinction data.

TABLE OF CONTENTS

I.	INTRODUCTION -----	8
II.	PROJECT BACKGROUND -----	10
III.	THEORY -----	19
	A. SCINTILLATION -----	19
	B. GAUSSIAN MODELLING -----	22
	C. EXTINCTION -----	27
IV.	INTERFACING -----	32
V.	COMPUTER PROGRAM DEVELOPMENT -----	38
	A. MODIFICATION OF THE ORIGINAL PROGRAM -----	38
	B. METEOROLOGY PROGRAMS -----	45
	APPENDIX A: INTERFACE LEAD CHART -----	55
	APPENDIX B: DATA STORAGE REGISTERS AND LABELS USED --	56
	APPENDIX C: CALCULATOR PROGRAM -----	58
	BIBLIOGRAPHY -----	71
	INITIAL DISTRIBUTION LIST -----	73

LIST OF DRAWINGS

1.	Photos of Mobile Optical Research Laboratory (bus) and the R/V Acania -----	13
2.	Photos of the Bus Telescope and the Gyro -----	14
3.	Photos of Meteorological and Optical Data Processing Equipment -----	15
4.	Early and Recent Scintillometers -----	18
5.	The Lognormal -----	24
6.	Photos of Interfaces -----	37
7.	Program Flow Chart -----	48
8.	Teletype Calibration Point Output and Photo of a Pulse-Height Analyzer Distribution -----	49
9.	Plotter Output of the Original Program -----	50
10.	Plotter Output of the New Program -----	51
11.	Printer Tapes from the Optical and Meteorological Programs -----	52
12.	Plotter Output - Gaussian Fit -----	53
13.	Plotter Output - Lorentzian Fit -----	54

ACKNOWLEDGMENT

The author wishes to express his appreciation to the students and professors of the atmospheric propagation group. A special note of gratitude is extended to Associate Professor Edmund A. Milne for his guidance and support and to Ellen for her love and patience.

I. INTRODUCTION

The potential utility of laser technology in the areas of line-of-sight communication, target tracking, and weaponry makes an understanding of the propagation of laser beams near the air-ocean interface imperative. The effects of a turbulent atmosphere on laser transmission were theoretically modelled by Tatarski [Ref. 1] et. al. and, subsequently, extensive field research in the terrestrial boundary layer has substantiated the bulk of the theory. Research data in the marine boundary layer has been scarce and inconclusive.

Atmospheric effects on laser propagation may be divided between laser-induced phenomena and those caused by meteorological characteristics independent of the laser's presence. The first classification applies only to lasers of sufficient power to heat the atmosphere (thermal blooming, upwind drift). The second is a universal grouping affecting the whole electromagnetic spectrum regardless of power. The atmospheric effects include beam refraction, beam spread (or degradation of resolution), absorption, and scattering. Refraction may be further categorized according to the dimensions of the atmospheric whirls. Large-scale vortices cause path deviation (beam wander) while small-scale vortices cause time-intensity variations (scintillation) and degradation of resolution.

The Naval Postgraduate School, Monterey, has been involved over the last four years in a continuing effort to establish the data base necessary to confirm or modify existing theory as applied to the air-ocean interface. Two research groups have operated simultaneously but independently; the optical research group and the atmospheric turbulence group have attempted to correlate determinations of C_N (the refractive index structure constant) through the respective analysis of light intensity distributions and meteorological data. The optical research group has concurrently investigated scintillation, extinction (scattering and absorption) and the atmospheric modulation transfer function (a measure of beam spread and wander). Theses on the effects of aperture averaging, determination of an atmospheric extinction constant, and determination of an atmospheric MTF for a black-body source were completed over the same period as the author's [Refs. 10, 11, 12].

A major problem for the optical group was the inordinate amount of time necessary to process scintillation and extinction data. The methods employed depended heavily on operator analysis of raw data or extensive manual input to computers. While the processing theory being applied was appropriate, the time penalty and the inherent high probability of error had to be minimized. The author concentrated his efforts in this area employing only the basic results of laser propagation theory.

II. PROJECT BACKGROUND

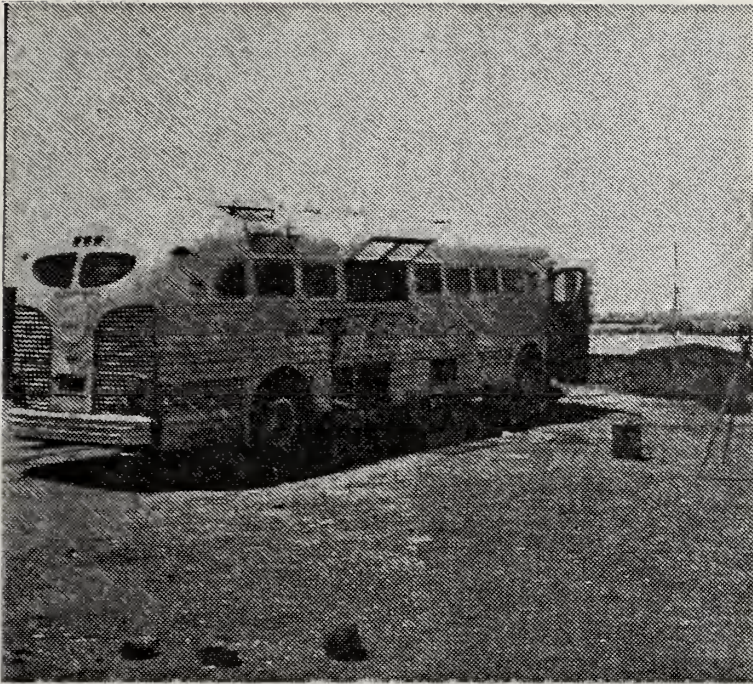
Various members of the Naval Postgraduate School's faculty have been conducting research on atmospheric propagation phenomena since 1972. The first experiments investigated the atmospheric MTF and scintillation in the basement corridor of Spanagel Hall. In the scintillation experiment a laser beam reflected from a flat mirror placed at the opposite end of the 137 meter passageway and entered a pin diode detector located near the laser source. The detector output, proportional to the incident beam intensity, was passed through a log-amplifier and recorded on magnetic tape. The data was later periodically sampled, digitized, and accumulated by a pulse-height analyzer; the resultant distribution was Gaussian, as theory had predicted. Refractive index structure constants were calculated from photographs of the distributions by measuring the curves' full width at half maximum height. The MTF measurement used a six inch parabolic mirror mounted as a Newtonian telescope. The image from a laser at the other end of the passageway was scanned across a slit using a cam-driven rocking diagonal mirror. The output of a photocell was fed to a boxcar integrator to generate time-averaged data, which was then recorded. Turbulence in the hall was somewhat controllable and detectable reduction of MTF with turbulence was observed.

In late 1972 a group of interested researchers discussed possible environmental experiments. The first such experiment was completed 10 January 1973 by faculty, staff, and students and involved shining a low-power (mW) red laser (6328 Å) across a 4.3 kilometer range at the southern end of Monterey Bay. The research vessel Acania was anchored at the approximate midpoint of the beam path to take atmospheric turbulence measurements with onboard sensors. In a second experiment at San Nicholas Island (3 March 1973) low power laser beams were transmitted from the northwest tip of the island to the Acania anchored offshore. The qualified success of these experiments completed with equipment already owned by the school was encouraging enough to prompt the submission of a research proposal to the Naval Ordnance Laboratory (White Oak, Md.) for fiscal year 1974.

Experimental apparatus has changed significantly since the Navy lab started sponsoring the research. A Cassegrainian telescope system with an eighteen inch parabolic mirror and an elastically mounted scanning mirror (driven electromagnetically by a shaped waveform) was used in the most recent MTF measurements. An enclosed trailer was built to transport and protect the telescope and associated equipment; aluminum support legs that extended to rest directly on the ground negated the previously persistent problem of telescope motion due to operator movement. More recently a bus has been used which holds most of the on-shore optical and meteorological

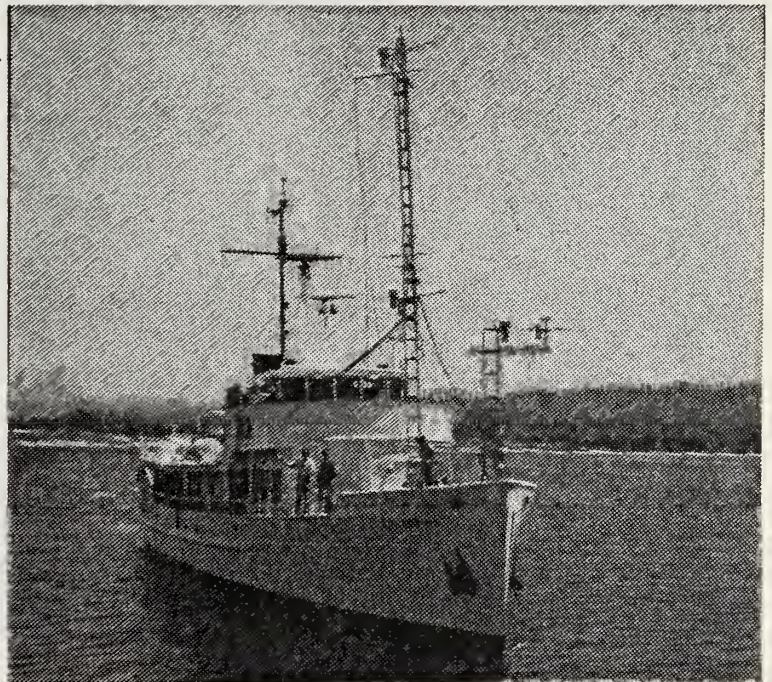
equipment and employs the same independent telescope suspension idea. Ship motion originally made it difficult to keep even a diverged laser beam on the telescope long enough to collect meaningful MTF data. A gyro-stabilized tracking system was designed to go aboard the Acania. At first it was manned by two operators who sight-aimed a gyro-mounted laser with hand-operated servo joy sticks; one controlled horizontal and the other the vertical train. Little useable data was obtained with this system because of problems with human coordination and fatigue. The solution was a quadrant detector servo system which will lock on a laser beam once the operator has aligned it with the target. Shipboard scintillation detectors are also mounted on the gyro frame and thereby maintain a constant relative position in the incident beam path. The gyro has been housed in an aluminum shed, when aboard the Acania, to protect both equipment and operator from the elements.

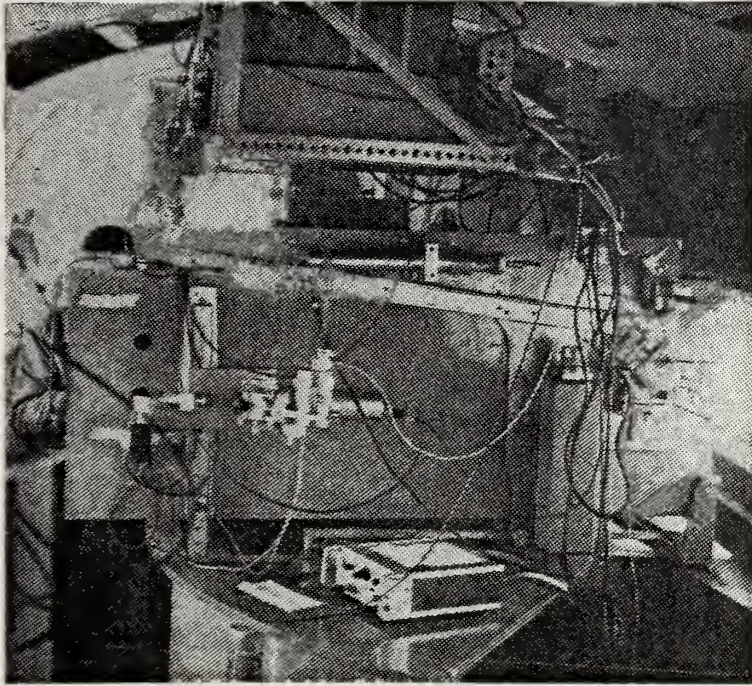
Scintillation data was best taken aboard the Acania; a detector with a wide angle of acceptance could continuously sample a diverged beam from ashore more readily than the reverse because of the effect ship motion would have on the direction of propagation of a beam originating on board. The single-detector system originally employed required excessive attention during data runs because light from environmental sources refracts into the beam path and can't be distinguished from that of the monitored laser. Since all



The bus with telescope in position. Transit to the right was used in range-to-ship calculation. In background stands meteorological tower supporting sensors.

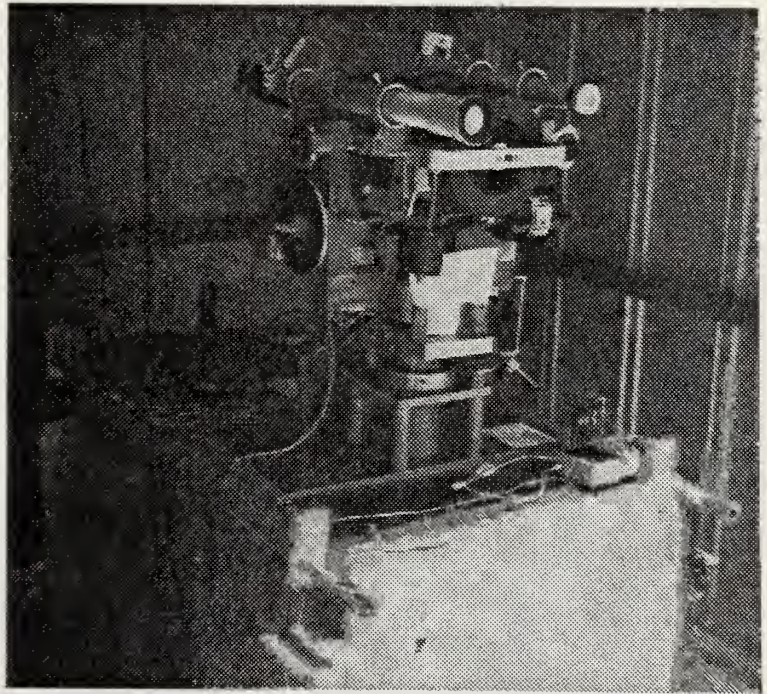
Naval Postgraduate Research Vessel Acania with meteorology gear deployed. The aluminum shed which shelters the gyro is aft of the pilot house.

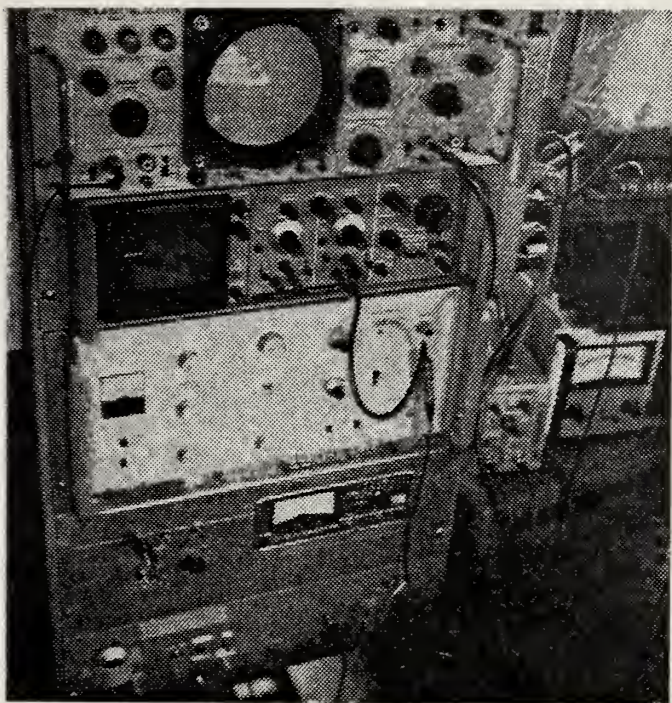




Right side of telescope showing fan-scan unit, laser, detectors, tracking unit, and associated electronic gear.

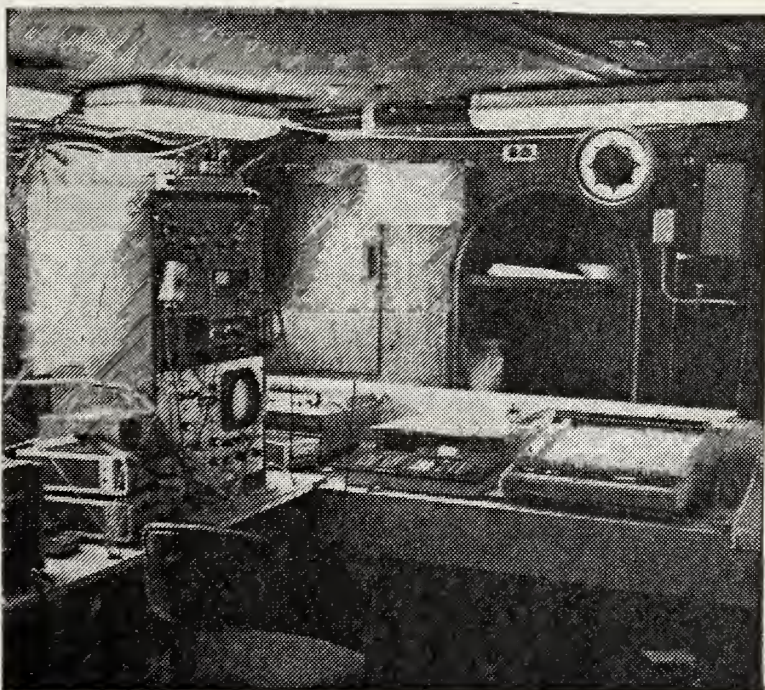
Gyro-stabilized tracking unit. The detectors are mounted on top and the lasers are hidden from view below.





Oscilloscopes,
Nuclear Data Analyzer,
log-amplifier, and
demodulator; here
shown set up for
meteorological data
processing on the
bus.

Dry lab on the
Acania with
scintillation/
extinction data
processing gear:
PIP-400, PAR
amplifiers,
demodulator, log-
converter, HP9810A
calculator and
plotter, Oscillo-
scope & freq
analysis tape
recorder.

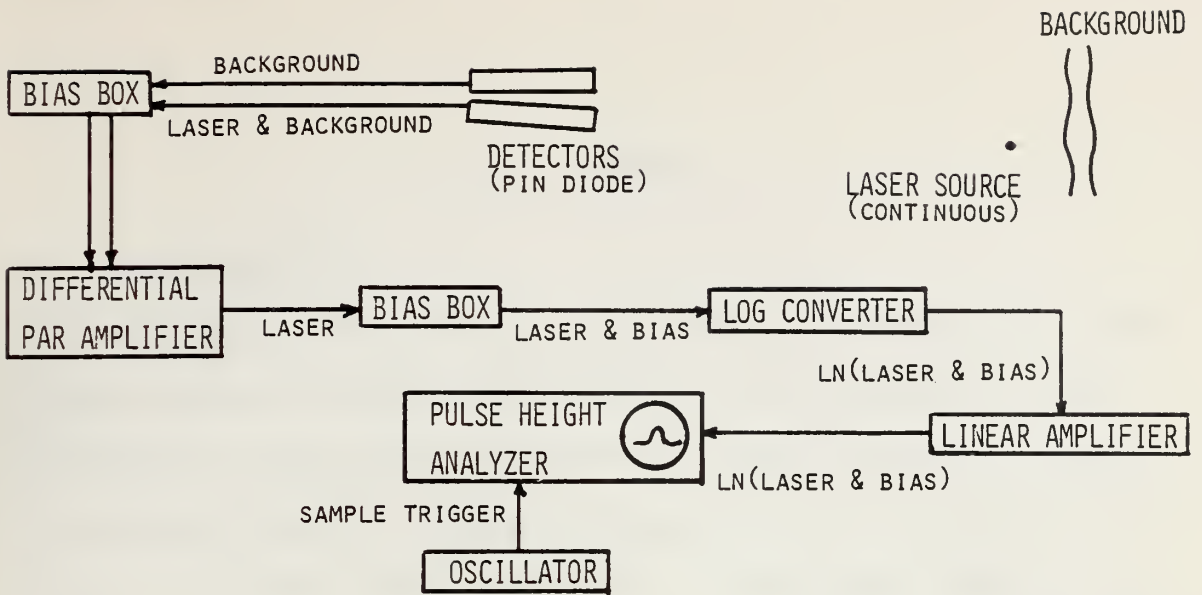


photocell data passed through a log-amplifier a skewed distribution would result. In an attempt to negate this effect the beam had to be interrupted ten seconds out of every minute to zero-out detector voltage generated by background radiation. A dual-detector system was built with the idea that the output of one pin diode detecting only background could be subtracted continuously from that of another unit aimed at the laser beam.

Since the detectors (supposedly identical) produced different proportional outputs extensive voltage biasing was necessary. An even greater problem was that ship motion continuously changed the position of the detector relative to the beam center. Subsequently another single-detector system was designed, this one employing a chopped laser source and a demodulator. The chopping was accomplished at the source by reflecting the laser light first off of a cylindrical mirror which fanned the beam horizontally and then off of a flat mirror vibrating at approximately two kilohertz which made the beam scan vertically. The demodulator unit took the detector output and electronically subtracted the minima (background) from the maxima (laser & background) and sent the difference to the log-converter. Detector sensitivity was recently increased by replacing the pin diode with an avalanche detector. An FET follower converts the high-impedance output of the detector to a low impedance which can be transmitted a greater distance through coaxial cable.

This has allowed all data processing gear on the Acania to be positioned below-decks in the dry lab.

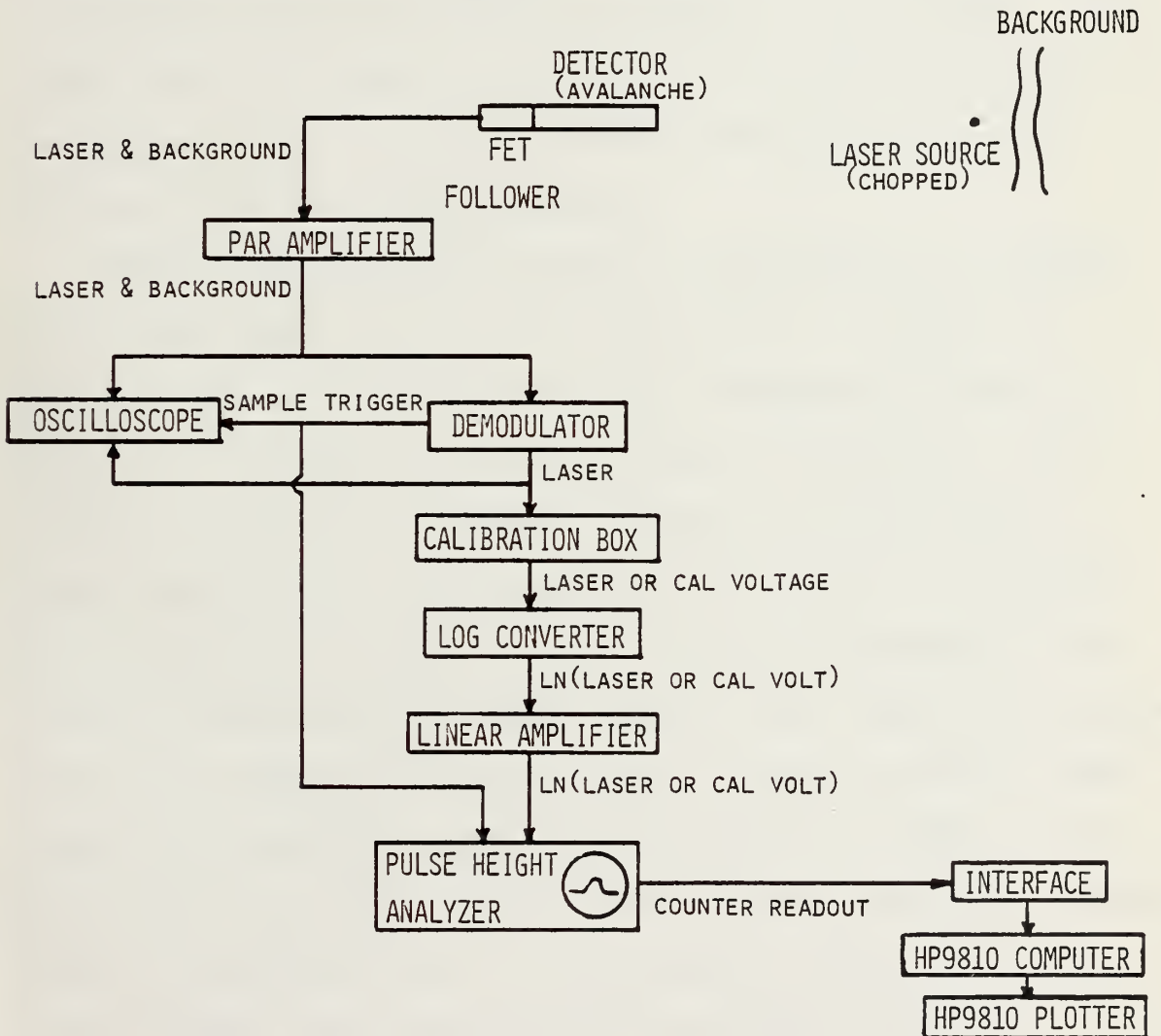
Processing of scintillation data was initially best accomplished through physical measurement of photographs of resultant distributions displayed on the PIP-400 pulse height analyzer. Attempts to record and subsequently analyze data with integral methods on a computer suffered from poor digitizing. Digital output could be obtained directly from the PIP-400 by a fast printer or from a Nuclear Data 128-channel analyzer by teletype. An attempt was made to fit a Gaussian curve to the data using least-squares method. This analysis proved highly successful when extraneous voltages did not skew the experimental distribution but was painfully slow because data had to be manually input to the computer point by point. The most recent improvement has been the direct interfacing of the PIP-400 with a compact computer programmed to process scintillation and extinction data on-scene within six minutes of sampling. This was completed by the author and is the subject of this thesis.



early

SCINTILLOMETERS

recent



III. THEORY

A. SCINTILLATION

The theory of optical propagation in a turbulent atmosphere has been extensively documented and those portions employed by the Naval Postgraduate School optical propagation group have not changed significantly since the project began. A thesis submitted by B. C. Haagensen [Ref. 3] in June, 1973 contained an excellent outline of the pertinent theoretical derivations and an extensive bibliography. The author does not intend to list or verify familiar theoretical developments but rather to present the significant end products vital to data processing.

Theory states that atmospheric turbulence is a random, non-linear, three-dimensional phenomenon. A turbule is ideally assumed to be an isotropic, homogeneous pocket or swirl of air with a particular index of refraction. The inertial subrange delineates a region of turbule size in which refraction is theoretically described; it is bounded on one side by turbules so small (a few millimeters) that viscous dissipation of energy causes their immediate collapse and on the other by eddies so large (order of meters) that they are no longer homogeneous and energy is added to the turbulence spectrum. In the inertial subrange large turbules form and transfer energy to successively smaller turbules with minimal losses through viscous dissipation.

Tatarski [Ref. 1] described the three-dimensional power spectral density of turbulence, $\Phi_n(K)$, with the equation:

$$\Phi_n(K) = 0.033 C_N^2 K^{-11/3} \exp \left[-\frac{K^2}{K_m^2} \right]$$

where:

C_N = refractive index structure constant

K = spatial wave number = $\frac{2\pi}{\ell}$

ℓ = coherence length of a turbule

$K_m = \frac{2\pi}{\ell_0}$; ℓ_0 = lower limit of inertial subrange

C_N obviously parameterizes the total amount of energy in the turbulence. The random distribution of turbulence cannot be forecast and must be described statistically. A beam is modulated in a multiplicative manner when it passes through successive turbules of differing index of refraction. It follows that the natural log of the beam intensity is altered additively and should follow a normal probability distribution as a result of the central limit theorem. C_N is directly related to the structure function of the refractive index (the mean square difference of the index of refraction at two points a distance d apart) by:

$$D_n(d) = \langle [n(r) - n(r+d)]^2 \rangle = C_N^2 d^{2/3}$$

After lengthy derivation and a number of assumptions [Ref. 4, pg. 10], C_N can be seen to be directly dependent on the variance of the log intensity distribution by:

$$C_N = 1.42 K^{-7/12} Z^{-11/12} C_{\ell I}$$

where

$$C_{\ell I}^2 = \langle [\ln(I) - \ln\langle I \rangle]^2 \rangle = \text{variance}$$

$$Z = \text{optical propagation path length}$$

C_N can also be calculated by a statistical determination of the temperature structure constant, C_T^2 , since temperature is the dominant factor in a meteorological formulation of the index of refraction:

$$C_N = (79.0 \frac{P}{T^2} \times 10^{-6}) C_T$$

where

$$P = \text{mean pressure in millibars}$$

$$T = \text{mean temperature in K}$$

$$C_T^2 = \frac{\langle [T(r) - T(r+d)]^2 \rangle}{d^{2/3}}$$

A major objective of the project is to study the correlation between C_N values obtained optically and meteorologically.

B. GAUSSIAN MODELLING

According to theory, periodic sampling of a laser beam propagating in the inertial subrange should approximate a lognormal distribution; if the natural log of the detector voltage (proportional to beam intensity) defines abscissa values and the ordinate marks the number of samples returning a specific voltage the resultant plot should be of the form:

$$y = C \exp \left[-\frac{(x - \bar{x})^2}{2\sigma^2} \right]$$

where:

C is a constant

x is natural log of detector voltage

\bar{x} is the average natural log of detector voltage

σ^2 is the variance ($C_{\ell I}^2$)

Taking the natural log of each side:

$$\ln y = -\frac{x^2}{2\sigma^2} + \frac{\bar{x}x}{\sigma^2} + (\ln C - \frac{\bar{x}^2}{2\sigma^2}) = ax^2 + bx + c$$

where:

$$a = - \frac{1}{2\sigma^2}$$

$$b = \frac{\bar{x}}{\sigma^2}$$

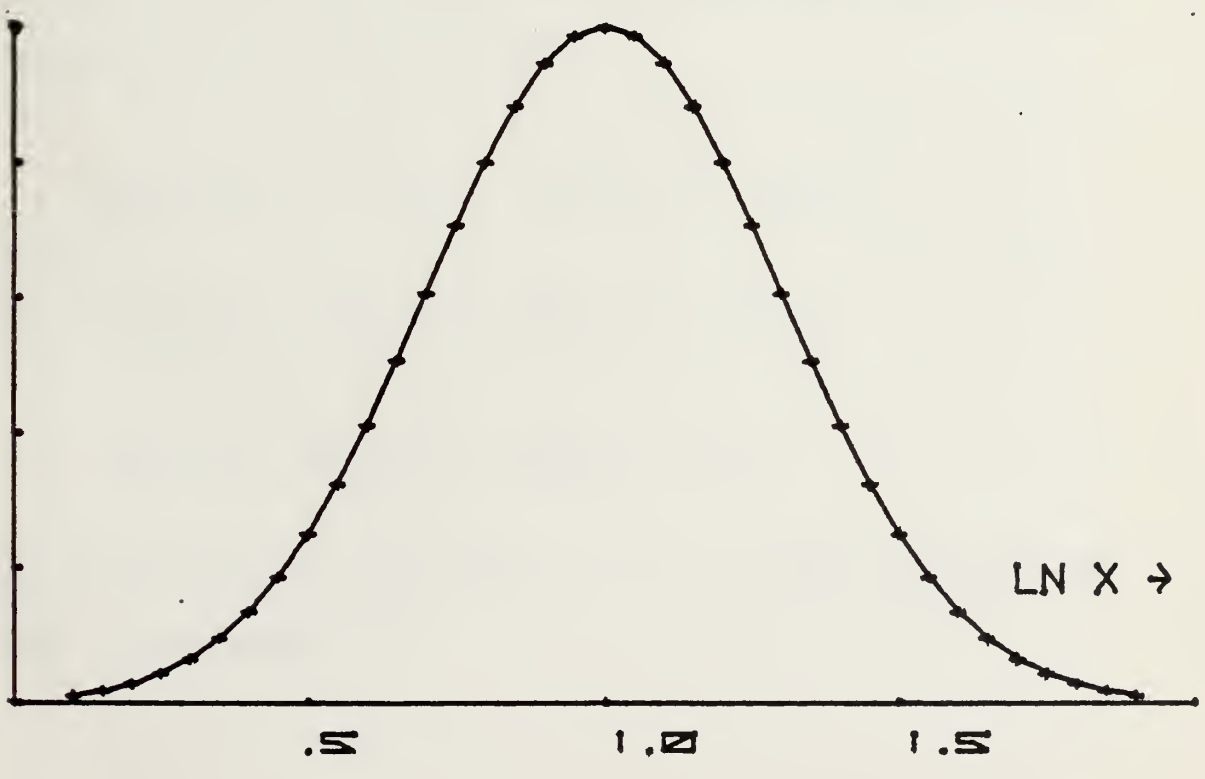
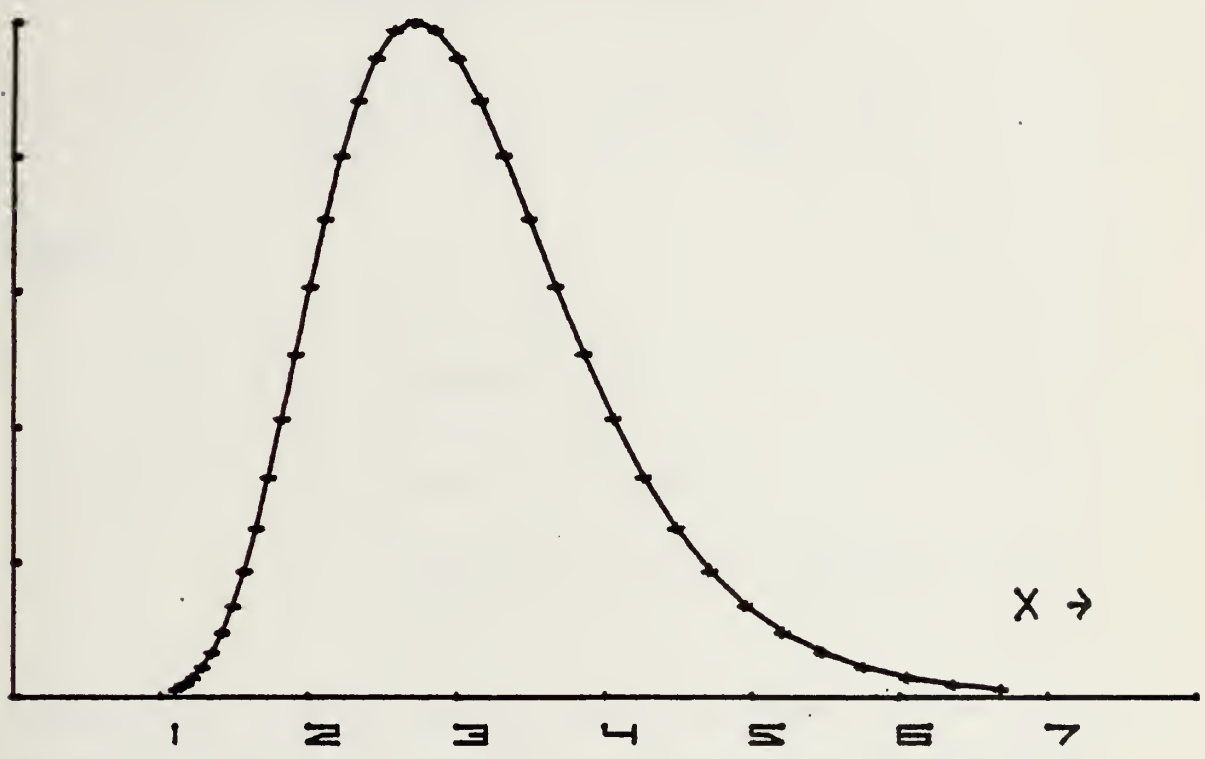
$$c = \ln C - \frac{\bar{x}^2}{2\sigma^2}$$

Experimentally the natural log of detector voltage axis is divided by the PIP-400 into two hundred channels of equal width and the y axis is the number of counts (or times) the equivalent detector voltage (or beam intensity) was detected over the sampling period. The number of counts in each channel after a data run can be assumed to be Poisson-distributed; for one measurement the 68% confidence interval is $y \pm \sqrt{y}$. Since the natural log of y is taken to obtain the quadratic form, the uncertainty in $\ln(y)$ becomes:

$$d[\ln(y)] = \frac{dy}{y} = \frac{\sqrt{y}}{y} = \frac{1}{\sqrt{y}} .$$

So, for the log distribution, the channels with the largest numbers of counts have the narrowest confidence intervals (smallest uncertainty) and should be weighted more heavily. The effect of narrowing confidence intervals with increasing counts is easily illustrated by plotting them on log paper. In the original program it had been decided to weight the data inversely with the uncertainty, i.e. multiply by \sqrt{y} .

THE LOGNORMAL



The $\ln(y)$ distribution resulting experimentally can be approximated with a polynomial by means of least-squares fitting. The method seeks to minimize

$$\sum_{i=0}^{199} w_i [\ln(y_i) - ax_i^2 - bx_i - c]^2$$

where:

x_i = channel number i

y_i = counts in channel i

w_i = weighting of data in channel i , $\sqrt{y_i}$

Setting the partial derivatives with respect to a , b , and c equal to zero and cancelling common terms gives three equations with three unknowns:

$$\sum w_i x_i^2 \ln y_i = a \sum w_i x_i^4 + b \sum w_i x_i^3 + c \sum w_i x_i^2$$

$$\sum w_i x_i \ln y_i = a \sum w_i x_i^3 + b \sum w_i x_i^2 + c \sum w_i x_i$$

$$\sum w_i \ln y_i = a \sum w_i x_i^2 + b \sum w_i x_i + c \sum w_i$$

Applying Cramer's Rule [Ref. 6] to the system determines the coefficients:

$$a = \frac{\det(A_1)}{\det(A)}$$

$$b = \frac{\det(A_2)}{\det(A)}$$

$$c = \frac{\det(A_3)}{\det(A)}$$

where

$$\begin{aligned} \det(A) = & \sum w_i x_i^4 \sum w_i x_i^2 \{ \sum w_i - \sum w_i x_i \} \\ & + \sum w_i x_i^3 \{ \sum w_i x_i^2 \sum w_i x_i - \sum w_i x_i^3 \sum w_i \} \\ & + \sum w_i x_i^2 \{ \sum w_i x_i^3 \sum w_i x_i - (\sum w_i x_i^2)^2 \} \end{aligned}$$

$$\begin{aligned} \det(A_1) = & \sum w_i x_i^3 \{ \sum w_i x_i \sum w_i \ln y_i - \sum w_i \sum w_i x_i \ln y_i \} \\ & + \sum w_i x_i^2 \{ \sum w_i x_i \sum w_i x_i \ln y_i - \sum w_i x_i^2 \sum w_i x_i^2 \ln y_i \} \\ & + \sum w_i x_i \{ \sum w_i x_i^2 \sum w_i x_i \ln y_i - \sum w_i x_i \sum w_i x_i^2 \ln y_i \} \end{aligned}$$

$$\begin{aligned} \det(A_2) = & \sum w_i x_i^4 \{ \sum w_i \sum w_i x_i \ln y_i - \sum w_i x_i \sum w_i \ln y_i \} \\ & + \sum w_i x_i^3 \{ \sum w_i x_i^2 \sum w_i \ln y_i - \sum w_i \sum w_i x_i^2 \ln y_i \} \\ & + \sum w_i x_i^2 \{ \sum w_i x_i \sum w_i x_i^2 \ln y_i - \sum w_i x_i^2 \sum w_i x_i \ln y_i \} \end{aligned}$$

$$\begin{aligned} \det(A_3) = & \sum w_i x_i^4 \{ \sum w_i x_i^2 \sum w_i \ln y_i - \sum w_i x_i \sum w_i x_i \\ & + \sum w_i x_i^3 \{ \sum w_i x_i \sum w_i x_i^2 \ln y_i - \sum w_i x_i^3 \sum w_i \ln y_i \} \\ & + \sum w_i x_i^2 \{ \sum w_i x_i^3 \sum w_i x_i \ln y_i - \sum w_i x_i^2 \sum w_i x_i^2 \ln y_i \} \end{aligned}$$

Exactly the same forms for the coefficients result from applying Gauss-Jordan elimination [Ref. 6]. A total of eight distinct weighted-data summations form the basic elements which combine to give the coefficients. Coefficient "a" and a channel number-to-log voltage conversion factor deliver the lognormal variance ($C_{\ell I}^2$) which, with the optical wavelength and range, determines the refractive index structure constant (C_N). Coefficients "a", "b", and the conversion factor fix the average log voltage value ($\bar{\ln}$

C. EXTINCTION

Extinction is the loss of time-averaged intensity with distance by a beam propagating through the atmosphere. No extinction measurements had been taken by the optical propagation group before September, 1975. Assuming an exponential dependence and spherical spreading, extinction can be represented by an equation of the form:

$$I = \frac{I_0 R_0^2}{R^2} \exp [-\mu(R - R_0)]$$

where:

I = intensity at distance R

I_0 = intensity at distance R_0

R_0 = some arbitrary standard distance

R = some arbitrary distance

μ = the extinction coefficient

An equivalent form of the equation is:

$$I = \frac{1}{R^2} [I_0 R_0^2 \exp(\mu R_0)] \exp(-\mu R)$$

If R_0 is some small distance (on the order of a meter), the exponential with R_0 approaches one and the above form can be simplified to:

$$I = \frac{C}{R^2} \exp(-\mu R)$$

where

$$C = I_0 R_0^2 \quad (\text{a measure of source intensity})$$

Taking the natural log of both sides:

$$\ln I = \ln C - 2 \ln R - \mu R$$

Solving for μ :

$$\mu = \frac{\ln C - 2 \ln R - \ln I}{R} = \frac{\ln\left(\frac{C}{IR^2}\right)}{R}$$

The constant C must be determined at the time of the experiment and the time-averaged intensity and range must be measured. Since detectors generate voltages proportional to the incident intensities, voltage can be substituted for intensity with meaningful results. Phil Parrish investigated the extinction constant (C) and coefficient (μ) in a concurrent thesis [Ref. 10].

A statistical analysis was done to determine the extinction coefficient's degree of sensitivity to error in C, R, and I:

$$\mu(C, R, I) = \frac{\ln C - 2 \ln R - \ln I}{R}$$

$$d\mu = \frac{\partial \mu}{\partial C} dC + \frac{\partial \mu}{\partial R} dR + \frac{\partial \mu}{\partial I} dI$$

$$\frac{\partial \mu}{\mu} = \frac{1}{\mu} \left\{ \left(\frac{\partial \mu}{\partial C} \right)^2 dC^2 + \left(\frac{\partial \mu}{\partial R} \right)^2 dR^2 + \left(\frac{\partial \mu}{\partial I} \right)^2 dI^2 \right\}^{1/2}$$

Checking sensitivity to error with the true value of μ assumed to be 1×10^{-3} :

$\frac{dC}{C}$	$\frac{dI}{I}$	$\frac{dR}{R}$	TRUE RANGE	$\frac{\delta\mu}{\mu}$ form	$\frac{\delta\mu}{\mu}$ value
0.01	0	0	1500 7500	$\pm \frac{dC}{\mu RC}$	0.007 0.001
0.10	0	0	1500 7500		0.067 0.013
0	0.01	0	1500 7500	$\pm \frac{dI}{\mu RI}$	0.007 0.001
0	0.10	0	1500 7500		0.067 0.013
0	0	0.01	1500 7500	$\pm (1 + \frac{2}{\mu R}) \frac{dR}{R}$	0.023 0.013
0	0	0.10	1500 7500		0.233 0.127
0.05	0.10	0.05	1500 7500	$\left\{ \frac{dC^2}{\mu^2 R^2 C^2} + \frac{(2 + \mu R)^2 dR^2}{\mu^2 R^4} + \frac{dI^2}{\mu^2 R^2 I^2} \right\}^{\frac{1}{2}}$	0.138 0.065

Obviously, errors in all quantities have more effect at shorter ranges. Errors in the extinction coefficient appear to depend linearly on independent errors in the extinction constant, time-average intensity, and range but decrease with increasing true range. Errors in range have a much greater effect than equivalent errors in either of the other quantities. The last two calculations in the previous table use maximum error values estimated to be appropriate with present equipment and procedure.

IV. INTERFACING

The fitting of normal distributions to scintillation data through a computer program using least-squares method had proven highly successful but also extremely slow. The PIP-400 pulse height analyzer used to accumulate data distributions had the design capability to output the information through a 50-pin plug in parallel BCD (binary coded decimal) readout. The HP9810A calculator in which the processing took place had an optional parallel input interface card which accepted BCD input through a 50-pin plug at the same voltage levels as put out by the PIP-400. It was thought that a simple interface matching the proper lines would obviate the pokey manual input of data. A number of hidden problems were found which made the project much more difficult than expected.

The first problem was that both machines had been designed as masters. The analyzer sent a high-to-low (voltage) print command and waited for a low-to-high flag from the peripheral (which told it to step to the next channel). The calculator sent a high-to-low voltage command to an external source asking for data and waited for a low-to-high flag which told it the information was ready. The solution was to invert both sets of signals so that the data request from the calculator appeared as a peripheral flag to the analyzer and a data print command from the PIP-400 appeared as an information

ready flag to the HP9810. If the analyzer function knob is set to "PRINT" before the calculator asks for data the first channel will be ignored, but since the first (and last) five channels of the distribution are zeroed by the program anyway (because of the high probability of extraneous counts in these channels) the deletion has negligible effect. Since the voltage signal levels for both machines matched, the modification was completed with a single hex inverter chip (Signetics 7404) using two of the six inverters available. A six volt supply lead from the analyzer and a 100-ohm resistor filled the inverter's power requirement ($5 \pm .25$ volts).

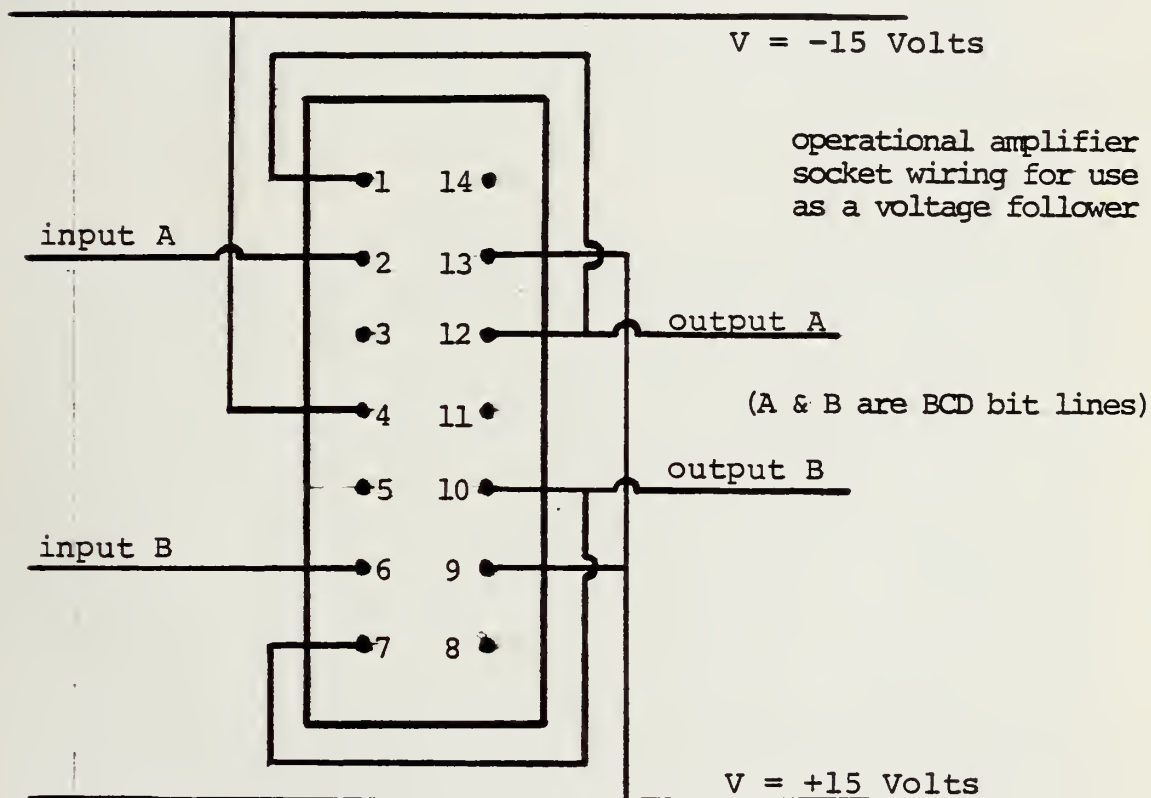
Matching the data lines proved more of a problem. Data from the analyzer in parallel readout consists of six data digits followed by three address digits. Digital information is relayed in BCD which requires four bitlines for each decimal digit. The PIP-400 puts out a low current, high impedance data signal while the HP9810 uses a pull-up resistor to bring an expected high current, low impedance signal up to five volts for a "1" bit. The calculator reads anything over 2.8 volts as a "1" bit and anything less as a "0" bit. With the command lines being inverted by the chip and the thirty-four information bit lines properly mated (inside a junction box with two 50-pin plugs) a calculator print-out of analyzer data showed all 9's; this meant that the pull-up resistor in the calculator was raising all

analyzer output signals to over 2.8 volts. This supposition was substantiated when the correct data was properly read out of the analyzer by a fast printer through the same output plug.

The first solution attempted was to install a grounded quarter-watt resistor in parallel with each signal line to pull the voltage of a "0" bit below 2.8 volts. The address numbers were successfully printed using a 5600 ohm resistor on each lead but the data digits were decidedly non-uniform in their individual bit resistor requirements. Comparison of calculator printouts with fast printer readouts were used to determine the necessary resistance; lead requirements varied between 4700 and 8200 ohms for the calculator to print data digits accurately. Variable (0 - 10,000 ohm) potentiometers were used to find the range of resistance values between those which fixed a bit's output at either "0" or "1". The proper resistance span was smaller, in some cases, than that separating successive standard resistors and was found to vary with time (possibly temperature dependent). Upon testing line voltage levels it was found that while the resistors brought a "0" bit from 3.0 to 2.7 volts it also brought a "1" bit down from 5.0 to 2.9 volts (approximate values). Since the fixed-resistor interface was obviously too finicky it was abandoned.

The next scheme attempted employed operational amplifiers (Signetics μ A747) constructed on silicon chips as unity-gain

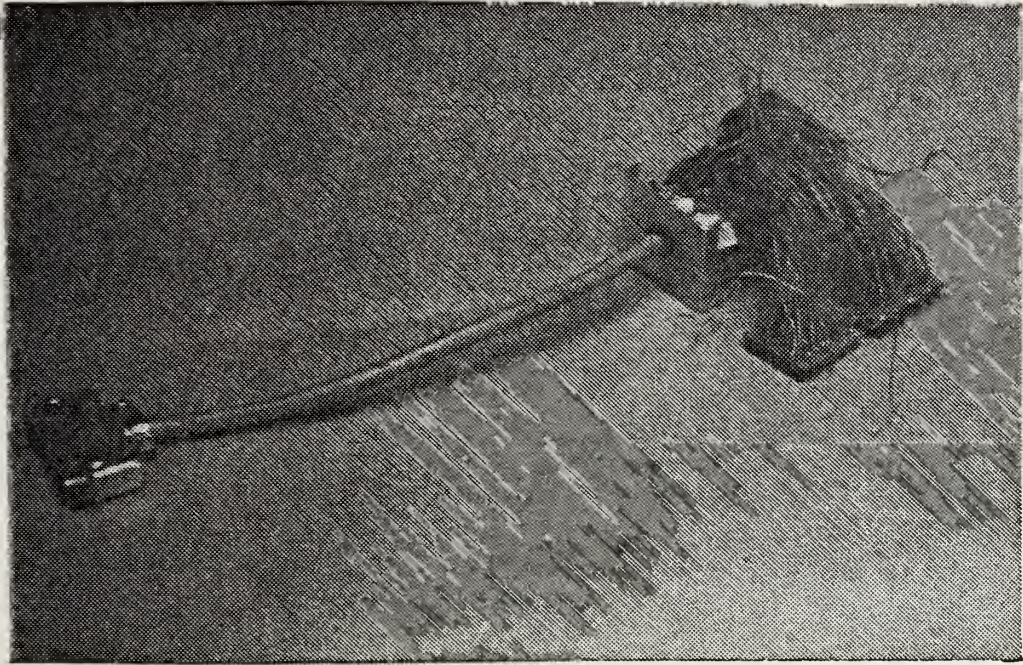
voltage followers and succeeded in generating the high current, low impedance input the calculator was designed to use. Seventeen op-amps were required to handle the thirty-four bits of information which made up each data point. The chips were all connected in parallel with a 100 mA dual power supply (run on 115 volt AC) which generated the ± 15 volts direct current necessary.



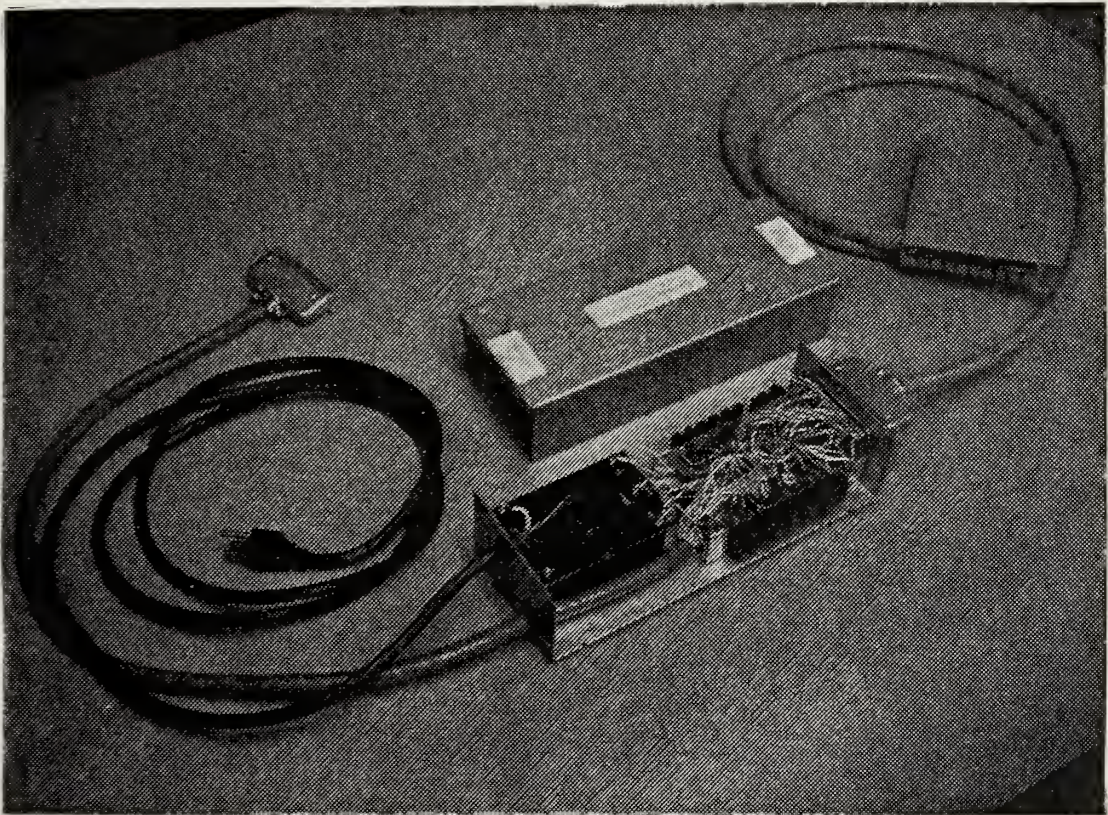
With the op-amps and additional wiring the circuitry was too bulky to be contained in the original junction box; after

the system had proven itself in the field it was redesigned and built with a junction box large enough to hold all the components internally.

The interfacing of analyzer and calculator cut the time to input each data point from seconds to milli-seconds; with a 200-channel analyzer (PIP-400) this meant a savings of five to ten minutes processing time on each run and made timely on-scene analysis of experimental distributions possible.



The remnants of the first interface using operational amplifiers. While successful it was too vulnerable in an operational environment.



The interface in its final form. To the right are the op-amps and inverter chip, to the left is the power supply. 50-pin plug on right goes to calculator, one on left to analyzer; outlet plug is for dual power supply.

V. COMPUTER PROGRAM DEVELOPMENT

A. MODIFICATION OF THE ORIGINAL PROGRAM

While mechanically interfacing the pulse height analyzer (PIP-400) and the computer (HP9810) saved a great amount of time previously used to input data, the computer program which processed the data was itself inefficient. An inordinate amount of time was spent labelling, giving operator instructions, and searching for subroutines. The program had been written in a straight-line manner with a minimal amount of branching for recurrent processes. The original program processed data for a least-squares fitting of a Gaussian and calculated the lognormal variance (SIGMA) and the refractive index structure constant (C_N) but did not compute the average detector voltage or an extinction coefficient. The program lacked the versatility to accept data from available analyzers by manual input.

The Hewlett-Packard 9810A calculator (with option 003 installed) has a total of 2036 locations in memory available for program steps of which 1847 were used in the original program. Since the additional desired processing could not possibly be accomplished in the steps remaining, a major program overhaul was required. The first measure taken was to delete or shorten as many labels and operator instructions as possible; approximately 250 program steps were excised in this manner with no functional loss. More steps were

saved by recording implemental constants on a magnetic card and entering them directly into the proper memory locations immediately after the program was loaded.

The program now had enough room for additional processing. In previous analysis [Ref. 3, et.al.) it was assumed that the natural log of the average detector voltage (beam intensity) was approximately equal to the average natural log of detector voltage. The validity of this assumption, initially made when computing the log-intensity variance with photographs, is crucial in extinction measurement (which depends on accurate determination of the average detector voltage). The immediate concern was the possibility of a functional relationship between average detector voltage (\bar{V}) and the exponential of the average log detector voltage ($\exp(\overline{\ln(V)})$) dependent on the average value ($\overline{\ln(V)}$) and the standard deviation (σ) of the lognormal distribution.

A computer program was developed which analyzed the variation of the ratio of the two quantities with increments of either $\overline{\ln(V)}$ or σ . The method was to assume an $\overline{\ln(V)}$ value for a Gaussian distribution and compute the average voltage. The probability density function of $\ln(V)$ was assumed, therefore, to be of the form:

$$y_{\ln} = C \exp\left[-\frac{(x - \bar{x})^2}{2\sigma^2}\right]$$

where:

$$x = \ln(V)$$

$$\bar{x} = \overline{\ln(V)}$$

Let $y(V)$ be the probability density function of V :

$$\int_a^b y_{\ln} dx = \frac{\exp(b)}{\exp(a)} \int y(V) dV$$

$$dx = d\{\ln(V)\} = \frac{dV}{V}$$

$$\therefore y_{\ln} dx = y_{\ln} \frac{dV}{V} = \frac{y_{\ln}}{V} dV$$

$$\int_{-\infty}^{\infty} y_{\ln} dx = \int_{\ln(0)}^{\ln(\infty)} \frac{y_{\ln}}{V} dV = \int_0^{\infty} y(V) dV$$

Since the number of total counts accumulated over a range of detector voltage while sampling will be identical whether the display distribution is linear or logarithmic:

$$y(V) dV = y_{\ln} dx = \frac{y_{\ln}}{V} dV$$

$$\therefore y(V) = \frac{y_{\ln}}{V} = \frac{C}{V} \exp\left[-\frac{(x-\bar{x})^2}{2\sigma^2}\right] = \frac{C}{V} \exp\left[-\frac{(\ln(V) - \overline{\ln(V)})^2}{2\sigma^2}\right]$$

Applying statistics:

$$\bar{V} = \frac{\int V y(V) dV}{\int y(V) dV}$$

For a normal distribution a dispersion index of $\pm 3\sigma$ gives a confidence limit of 99.73% [Ref. 7, et.al.) and these limits were imposed in a program applying Weddle's rule [Ref. 8] to accomplish the integration. The ratio of \bar{V} to $\exp(\overline{\ln(V)})$ was found to be independent of $\overline{\ln(V)}$ but an increasing function of σ . With points generated by the program (for σ values between 0.1 and 1.2 at increments of 0.02) a fourth-degree polynomial was found (using least-squares fitting) to generate average detector voltage values from average log-intensity. The polynomial coefficients were entered on the magnetic card carrying program constants and used to find the average detector voltage after determining $\overline{\ln(V)}$ (from the coefficients of the least-squares polynomial fitting data to a lognormal distribution). An easier method was subsequently employed which can be justified by proceeding further with the preceding derivation.

$$\bar{V} = \frac{\int V y(V) dV}{\int y(V) dV}$$

but

$$V = \exp(\ln(V)) = \exp(x)$$

and

$$y(V) dV = y_{\ln} dx$$

$$\therefore \bar{V} = \frac{\int \exp(x) y_{\ln} dx}{\int y_{\ln} dx} = \frac{\int C \exp(x) \exp\left[-\frac{(x-\bar{x})^2}{2\sigma^2}\right] dx}{\int C \exp\left[-\frac{(x-\bar{x})^2}{2\sigma^2}\right] dx}$$

After combining exponentials and completing the square in the numerator, and defining $x' = \bar{x} - \sigma^2$:

$$\bar{V} = \frac{C \exp\left(\bar{x} + \frac{\sigma^2}{2}\right) \int \exp\left[-\frac{(x-x')^2}{2\sigma^2}\right] dx}{C \int \exp\left[-\frac{(x-\bar{x})^2}{2\sigma^2}\right] dx}$$

The integrands in numerator and denominator are Gaussian distributions with the same standard deviations and, therefore, the same areas.

$$\therefore \bar{V} = \exp\left(\bar{x} + \frac{\sigma^2}{2}\right) = \exp(\overline{\ln(\bar{V})}) \exp\left(\frac{\sigma^2}{2}\right)$$

This derived result can be found in meticulous statistical literature [Ref. 9]. Since $\overline{\ln(\bar{V})}$ and σ were already available in the program the necessary calculation was easily included and required significantly less memory than the fourth-degree polynomial conversion. Incidentally, it was found that the polynomial method was accurate within 2% for standard deviation values between 0.1 and 0.9!

With an assumed extinction constant the calculation of an extinction coefficient is easily made, i.e.:

$$\mu = \frac{\ln\left(\frac{C}{\bar{V}R^2}\right)}{R}$$

where:

μ = extinction coefficient

C = extinction constant ($V_0 R_0^2$)

\bar{V} = average detector voltage

R = range

This computation was added to the program with the extinction constant becoming one of the operator input parameters.

The next program modification was the addition of a section which could process linear data to find the average detector voltage and extinction coefficient. The main purpose was to correlate results with those from the logarithmic section but this was not done to any great extent. The average channel number is determined by dividing the summation of channel number times channel counts by the summation of counts. The average channel number is then modified in a linear scaling process to give the average voltage. The extinction coefficient was computed in exactly the same way as in the logarithmic section.

After the linear portion was added the program almost filled available memory and was found to execute more slowly than before - especially plotting data. The program showed minimal utilization of subroutines and, consequently, the program wasted memory. The subroutines used were scattered throughout the body of the program which meant wasted time

spent searching after branching statements. The computer still took data input only from the PIP-400 through the interface. A Nuclear Data 128 channel analyzer which interfaced with a teletype was available as a back-up but the program had to be modified to accept manual input and a different channel capacity. With all the discrepancies a major reorganization was needed.

The HP9810A calculator branches to subroutines by going to the program beginning and searching through until finding the called label. This requires an inordinate amount of time to complete "do-loops" and subroutines. This problem was solved by making processes which were reiterative or used by more than one section of the program into subroutines and placing them in front of the main body. "Flag" statements were used to allow automatic or manual data input from the PIP-400 or Nuclear Data analyzer respectively.

The original program used a large amount of memory in a calculation to filter out bias introduced in the scintillometer. When the single-detector system for a chopped laser source was first put together the demodulator would output a few tenths of a volt with no input present thus biasing the sample distribution. This offset had to be taken into account when processing data because of its effect when using the logarithmic scale. In subsequent demodulators the offset problem was solved and the calculation became extraneous. When the process was removed from the program

the only discernable difference was an increased speed in plotting data.

The net result of all the program modifications previously discussed was a drop in the average processing time of an experimental distribution from over ten minutes to less than six minutes.

B. METEOROLOGY PROGRAMS

Just prior to the most recent R/V Acania experiments (May, 1976) Professor Schacher (associated with the atmospheric turbulence group) requested a computer program to fit a Gaussian curve to data manually input from the Nuclear Data pulse height analyzer. No explanation of the relevant theory was given or required to distill the necessary processing from the existing scintillation/extinction program.

Upon analyzing the processed data it was found that the Gaussian fit was a poor one. Prof. Schacher suggested the resultant data distributions appeared more Lorentzian and requested another program fitting data to that distribution.

The Lorentzian distribution is of the form:

$$y = \frac{A}{\Gamma^2 + (x-\bar{x})^2} = \frac{A}{x^2 - 2\bar{x}x + \bar{x}^2 + \Gamma^2}$$
$$\therefore \frac{1}{y} = \frac{1}{A} x^2 - \frac{2\bar{x}}{A} x + \frac{\bar{x}^2 + \Gamma^2}{A}$$

This can again be fitted by least-squares method to a quadratic and the coefficients evaluated to get the average

voltage (after scaling \bar{x} , the average channel number) and Γ (after scaling). The weighting scheme differed from that used for the Gaussian. The uncertainty is (again assuming the number of counts in each channel is Poisson-distributed):

$$d\left(\frac{1}{y}\right) = -y^{-2}dy = \frac{-dy}{y^2} = \frac{-\sqrt{y}}{y^2} = -y^{-3/2}$$

Again the data was weighted inversely with its uncertainty (multiplied by the number of counts in the channel to the 3/2 power). The least-squares fit attempts to minimize:

$$\sum \omega_i \left(\frac{1}{y_i} - ax_i^2 - bx_i - c \right)$$

where

$$\omega_i = y_i^{3/2}$$

$$y_i = \text{number of counts in channel } i$$

$$x_i = \text{channel number } i$$

$$a = \frac{1}{A}$$

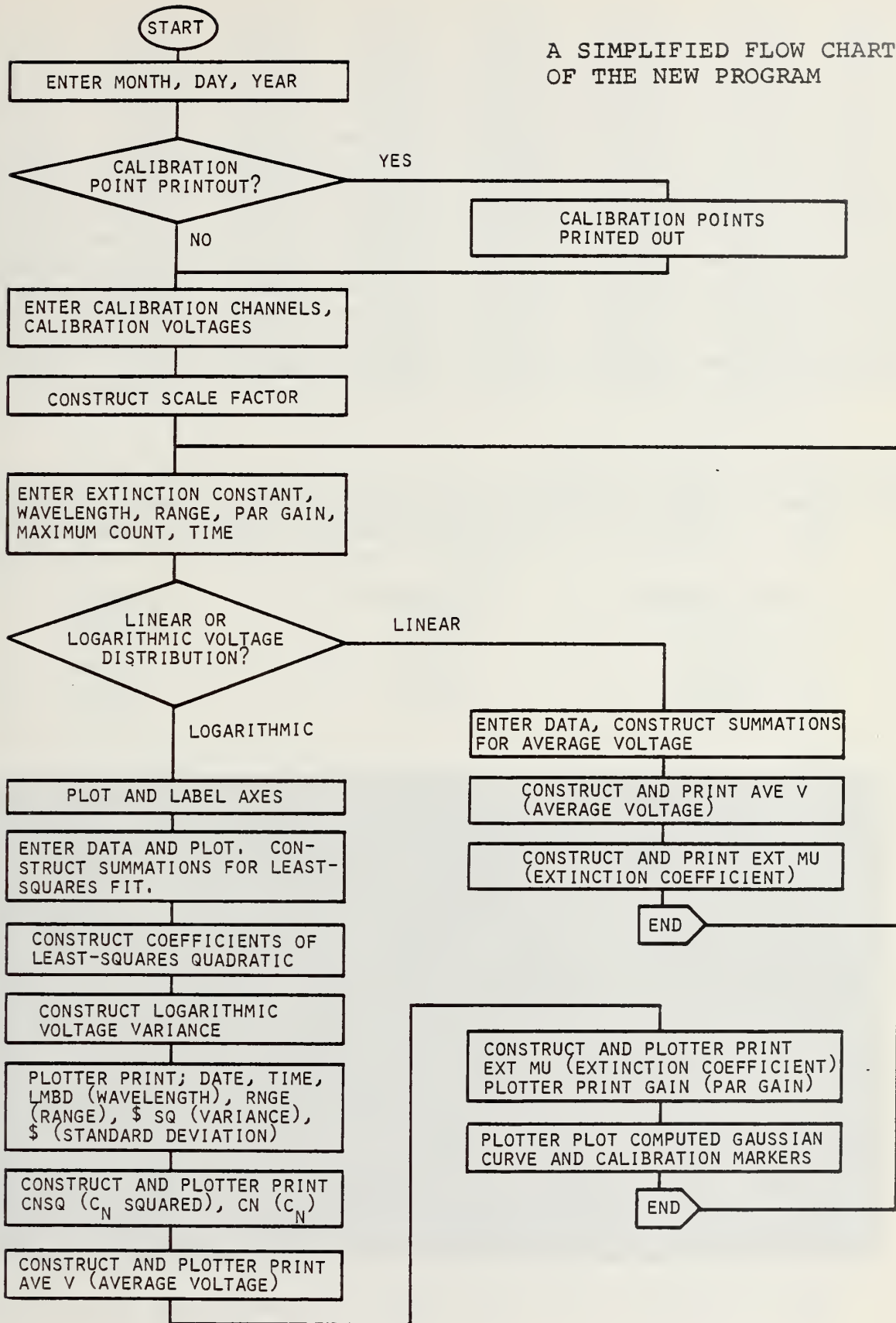
$$b = \frac{-2\bar{x}}{A}$$

$$c = \frac{\bar{x}^2 + \Gamma^2}{A}$$

Since all the machinery of the least-squares fitting of a quadratic applying Cramer's rule already existed, it was

a relatively simple matter to modify the existing Gaussian program. The comparative results definitely point to a Lorentzian distribution, which was not predicted by theory.

A SIMPLIFIED FLOW CHART
OF THE NEW PROGRAM



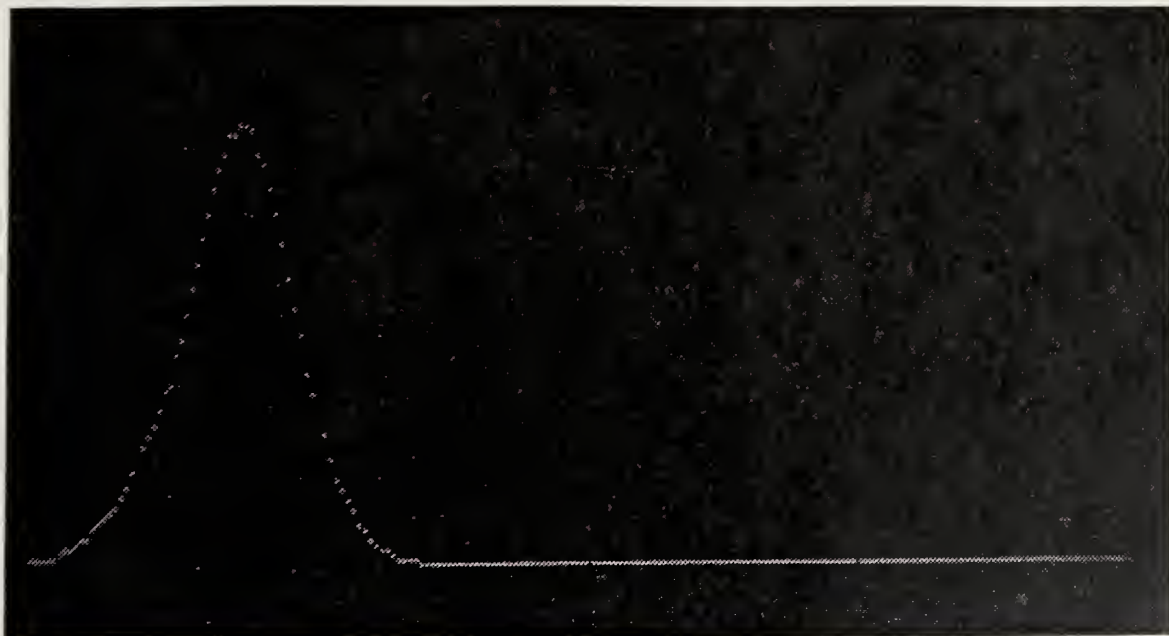
```

001034 *000000 *000001 *000000 *000000 *000001 *000000 *000000
000000 *000000 *000000 *000000 *000000 *000000 *000000 *000000
000000 *000000 *000000 *000000 *000000 *000000 *000000 *000000
000000 *000000 *000000 *000000 *000000 *000000 *000000 *000000
006291 *008860 *005971 *000000 *000000 *000000 *000000 *000000
000000 *000000 *000000 *000000 *000000 *000000 *000000 *000001
000000 *000000 *000000 *000001 *009367 *016270 *000002 *000000
000000 *000000 *000000 *000000 *000000 *000000 *000000 *000000
000000 *000000 *000000 *000000 *000000 *000000 *000000 *000007
006638 *003506 *000000 *000000 *000000 *000000 *000000 *000000
000000 *000000 *000000 *000000 *000000 *000000 *000000 *000000
000000 *000000 *000000 *006799 *002922 *000000 *000000 *000000
000000 *000000 *000000 *000000 *000000 *000000 *000000 *000000
000000 *000000 *000000 *000000 *000000 *000121 *007691 *003369
000000 *000000 *000000 *000000 *000000 *000000 *000000 *000000
000000 *000000 *000000 *000000 *000000 *000000 *000000 *000000

```

An example of the teletype output of the voltage calibration channel numbers used in scaling (reproduced from 1 March 1976). Notice the extraneous counts collected in channel 1. The points would be entered as follows:

<u>Voltage</u>	<u>Channel #</u>	<u>Change in #</u>
0.25	32.97	
0.50	52.63	19.60
1.00	72.35	19.72
2.00	91.30	18.95
4.00	110.30	19.00



PICTURE OF EXPERIMENTAL DISTRIBUTION AS DISPLAYED ON THE PIP-400 PULSE HEIGHT ANALYZER

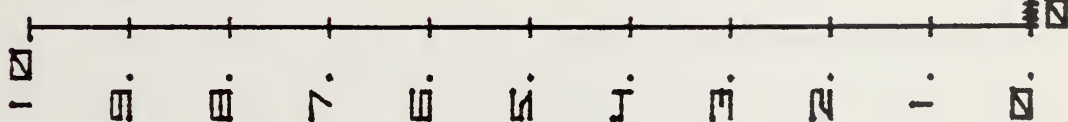
DATE 2./7./76. TIME 1245.

10 PT PINDS TO ACRANIA

WAVELENGTH = 0.6328 RANGE = 900.

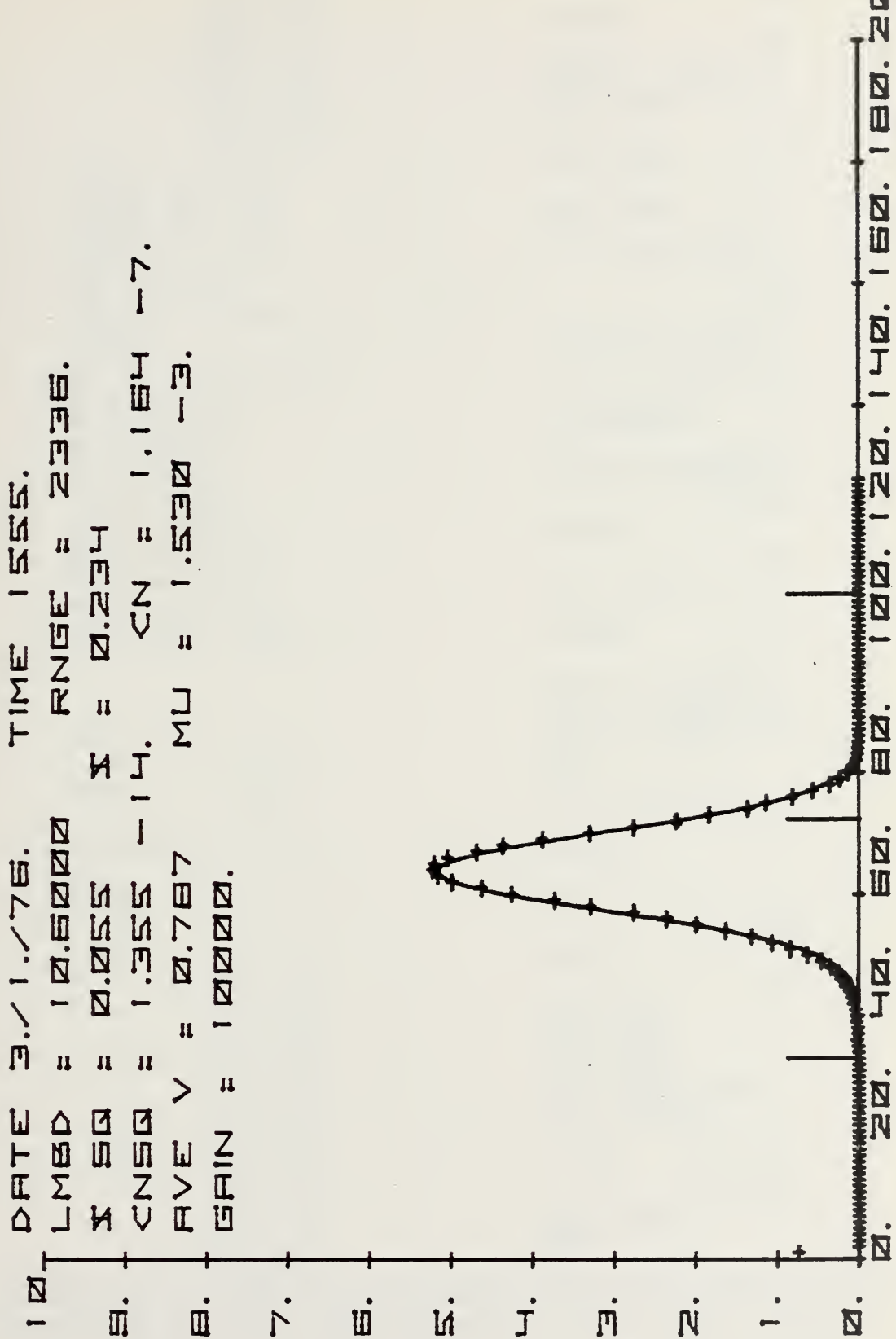
SIGMA SQUARED = 0.061 SIGMA = 0.248

CNSQ = 3.258 -15. CN = 5.708 -8.



AN EXAMPLE OF PLOTTER OUTPUT FROM THE OLD PROGRAM

DATE 3./1./76. TIME 1555.
 LMBD = 10.6000 RANGE = 2336.
 X SQ = 0.055 X = 0.234
 CNEQ = 1.355 -14. CN = 1.164 -7.
 AVE V = 0.787 MU = 1.530 -3.
 GAIN = 10000.



AN EXAMPLE OF PLOTTER OUTPUT FROM THE NEW PROGRAM

SET FLAG FOR
 CAL PRINTOUT
 11701.073
 3117.074
 7040.103
 10768.104
 10883.134
 10939.164
 8756.194
 2194.195

ENTER 1ST CAL
 ENTER 2ND CAL
 ENTER 3RD CAL
 ENTER V1 IN Y
 AND V3 IN X
 ENTER VOLTAGE
 OFFSET
 ENTER WAVELENGTH
 IN MICRONS
 ENTER RANGE
 IN METERS
 ENTER DATE
 ENTER TIME
 SET ANALYZER TO
 PRINT OUT AND
 SET FLAG FOR
 DATA PRINT OUT
 ENTER MAX COUNT

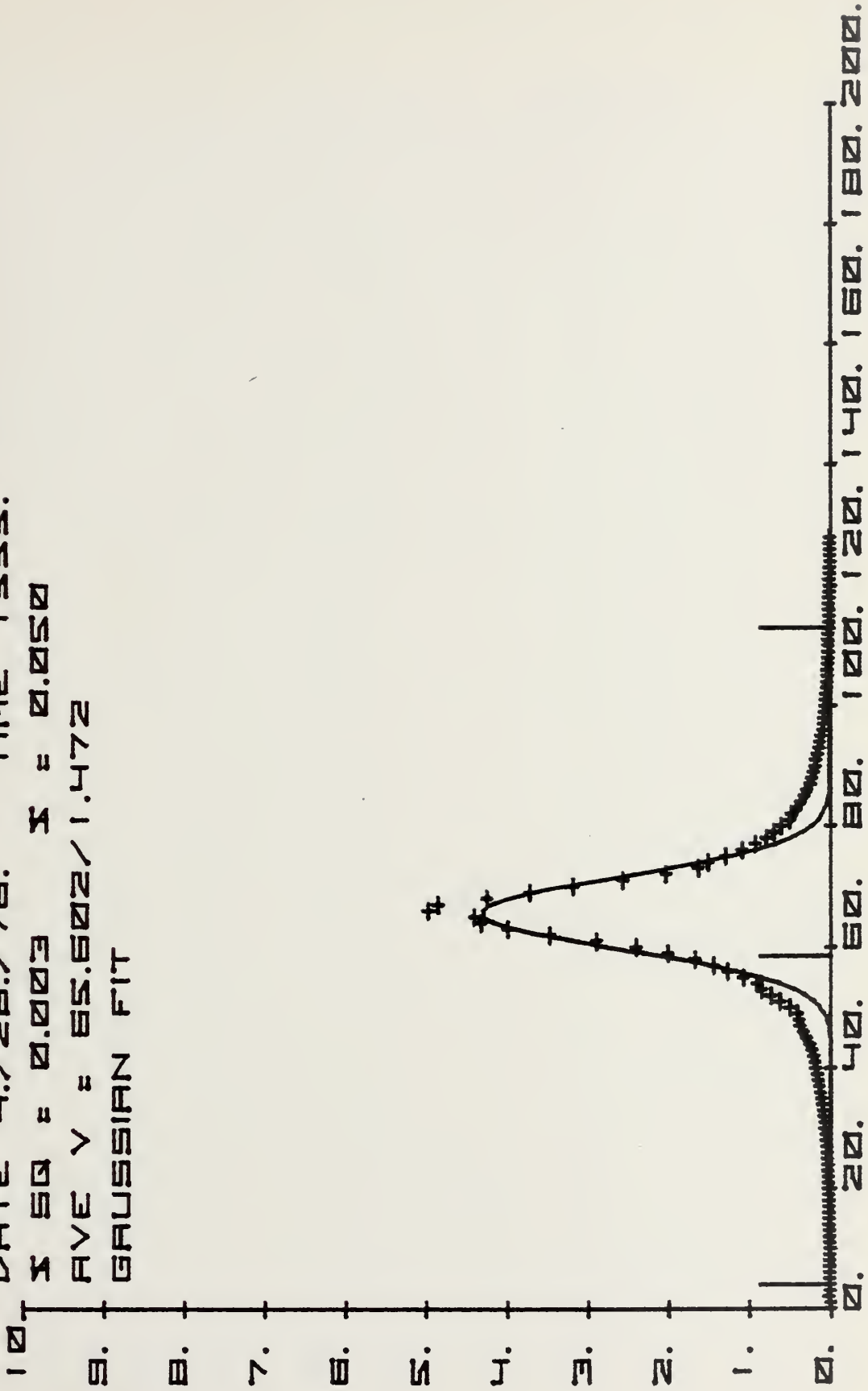
DATE
 20776.
 TIME
 1245.
 WAVELENGTH
 0.6328
 RANGE
 900.
 183.092
 291.093
 503.094
 569.095
 645.096
 640.097
 579.098
 758.099
 714.100
 767.101
 849.102
 (etc)

MONTH?
 4.
 DAY?
 30.
 YEAR?
 76.
 FLAG - CAL PTS
 1ST CAL?
 61.0
 2ND CAL?
 117.0
 3RD CAL?
 173.0
 V1-Y AND V3-X
 0.50
 8.00
 EXTINGUISH CONST?
 15300.00
 WAVELENGTH
 (MICRONS)?
 0.6328
 RANGE (METERS)?
 1625.
 GAIN?
 200.
 MAX COUNT?
 8000.
 TIME?
 1311.
 FLAG - LINEAR
 FLAG - LOAD DATA
 PIP ON PRINT?
 END

MONTH?
 4.
 DAY?
 28.
 YEAR?
 76.
 1ST CAL?
 2ND CAL?
 3RD CAL?
 V1-Y AND V3-X
 MAX COUNT?
 80000.00
 TIME?
 1555.00
 LOAD DATA
 END

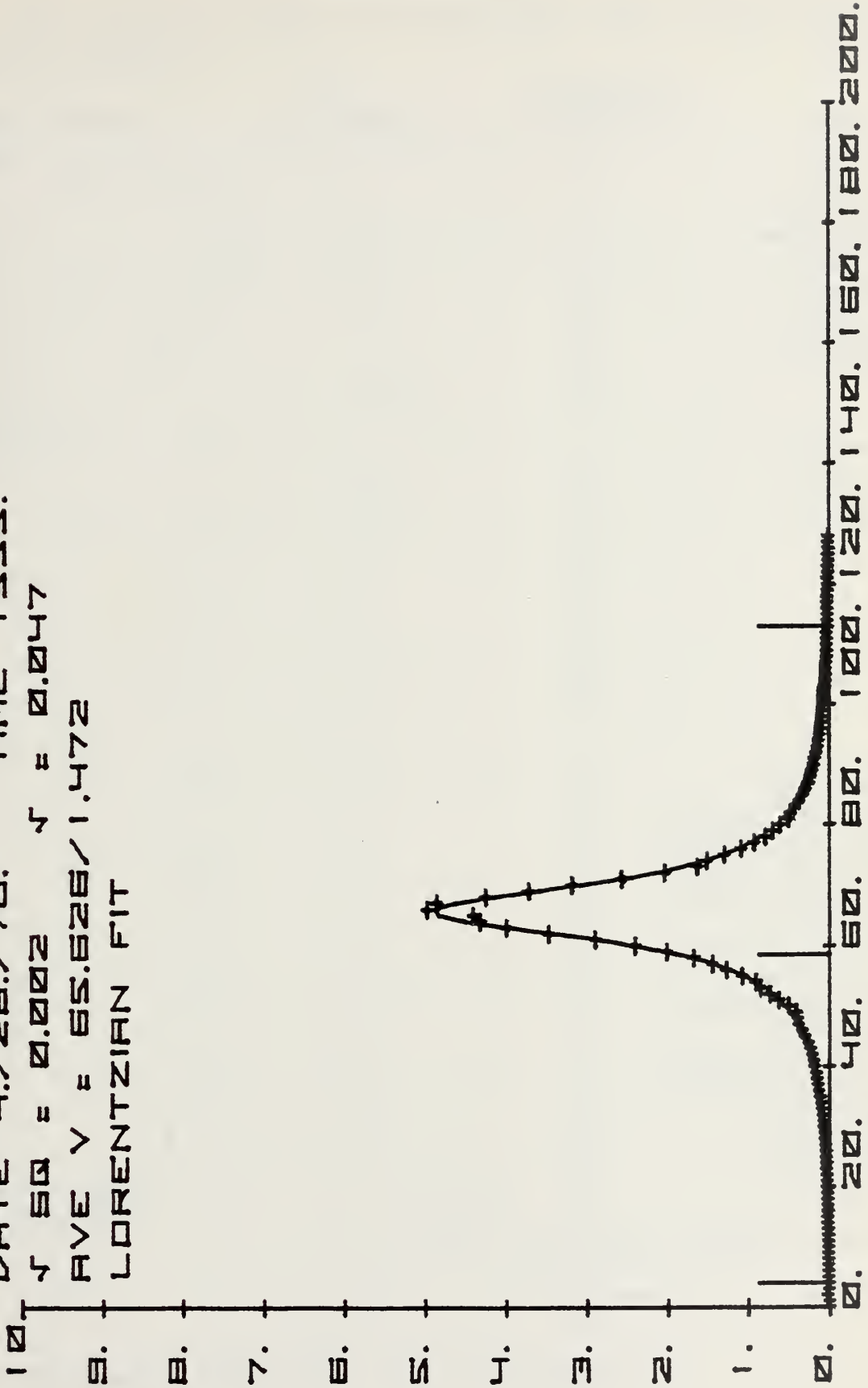
Reproductions of computer printer tapes made during data processing: original program with cal and data printout (left), present program (upper rt.), meteorology program

DATE 4./28./76. TIME 1555.
 Σ SQ = 0.003 Σ X = 0.050
 AVE Y = 85.602/1.472
 GAUSSIAN FIT



AN EXAMPLE OF PLOTTER OUTPUT FROM THE METEOROLOGY PROGRAM

DATE 4./28./78. TIME 1555.
 $\sqrt{SQ} = 0.002$ $\sqrt{\quad} = 0.047$
 AVE $\gamma = 65.626/1.472$
 LORENTZIAN FIT



AN EXAMPLE OF PLOTTER OUTPUT FROM THE METEOROLOGY PROGRAM

APPENDIX A

The following lists the connections made in mating the output plug of the PIP-400 to the input plug of the interface for the HP9810A:

<u>LEAD FUNCTION</u>	<u>PIP LEAD #</u>	<u>CALCULATOR LEAD #</u>	<u>COLOR</u>
DATA			
10 ⁵ - bit 1	1	6	red
" 2	2	7	white/black
" 4	3	8	white/green
" 8	4	9	blue
10 ⁴ - 1 bit	5	10	white/blue
2 "	6	11	green
4 "	7	12	white/gray
8 "	8	13	yellow
	9-12	N/C	
ADDRESS			
10 ² - 1 bit	13	30	white
2 "	14	31	white
	15,16	N/C	
10 ¹ - 1 bit	17	34	white
2 "	18	35	"
4 "	19	36	"
8 "	20	37	"
10 ⁰ - 1 bit	21	38	white
2 "	22	39	"
4 "	23	40	"
8 "	24	41	"
DATA			
10 ³ - 1 bit	25	14	white/violet
2 "	26	15	white/black(2)
4 "	27	16	white/yellow/black
8 "	28	17	white/blue/black
10 ² - 1 bit	29	18	white/red/black
2 "	30	19	white/orange/black
4 "	31	20	black
8 "	32	21	white/gray/black
10 ¹ - 1 bit	33	22	white/yellow
2 "	34	23	white/brown/black
4 "	35	24	white/orange
8 "	36	25	white/green/black
10 ⁰ - 1 bit	37	26	white/violet/black
2 "	38	27	white/red
4 "	39	28	white/brown
8 "	40	29	white/black
Print Command	41 inverted	49	white
Hold Command	42 "	47	"
Ground	43 chassis and power supply		white
	44-48	N/C	
+ 6 volts	49	hex inverter	white
	50	N/C	

N/C designates leads which are not connected

APPENDIX B

The following is a listing of the data storage registers utilized by the program:

<u>REGISTER</u>	<u>USE</u>
000	computed average logarithm of detector voltage
001	
002	
003	
004	computed summations for least-squares fit; 001,
005	002 and 003 are used subsequently to store the
006	coefficients of the least-squares polynomial
007	
008	
009**	9999
010	
011	determinants (formed from summations) which give
012	coefficients of the least-squares polynomial
013	
014	computed standard deviation of least-squares Gaussian fitted to data
021*	first calibration channel number
022*	second " " "
023*	third " " "
025	computed variance of least-squares Gaussian, later used again in C_N calculation
028*	time
030	wavelength in meters
031*	range in meters
041*	wavelength in microns
050	used in C_N calculation
051*	month
052*	day
053*	year
054	5/max count*
055*	gain
056*	extinction constant
057	computed average detector voltage
058	computed extinction constant
060	data point
061	data point weighting
065	channel number-to-voltage scaling constant
068	do-loop accumulators for the linear calculation
069	of average detector voltage
078*	first calibration voltage
079*	third " "
095	varying pen coordinate value for axis labelling
097	incremental pen coordinace values for axis labelling
098	label values in axis labelling
099**	236 (range of x-axis)
100**	11.8 (range of y-axis)
102**	alpha scale factor (0.1, FMT 11)
103	computer-scaled x-coordinate
104	" y-coordinate

<u>REGISTER</u>	<u>USE</u>
105**	-0.9 (Y_{\min}) (followed by FMT 13)
106**	10.9 (Y_{\min})
107**	-18 (X_{\max}) (followed by FMT 12)
108**	218 (X_{\min})
a & b	used many times through out the program

- * marks those registers whose values are input by the operator
- ** marks those registers with values stored on a magnetic card

The following is a list of label titles in the order they appear in the program:

<u>LABEL</u>	<u>FUNCTION</u>
A*(UP, DN)	takes manual or interface input; puts data in 060, channel in a, 5/max count in b
B*(1,2)	puts channel number in y and upper data channel limit in x
C*(3,4)	puts channel number in y and upper channel limit in x
D*(A,B,C,5)	plots data points and constructs summations necessary for least-squares fitting
E*(F)	plots the computed Gaussian and calibration points
F*	plots marker at calibration point
G*	constructs a special floating point form of a number to be plotted
H*(6,7)	labels plotted x & y axes
I*	computes the extinction coefficient
J*	prints operator instructions: FLAG - LOAD DATA; PIP ON PRINT?
K*	lists calibration points
L(K)	preliminary program set-up (month, day, year, calibration points, extinction constant)
M(N,H,J,D, G,I,E)	completes program set-up (wavelength, range, gain, max count, time); branches to label N for linear; plots and labels x & y axes; plots data; calculates desired constants; plots constants, computed Gaussian, and calibration points; returns to label M
N(J,A,B,I, M,8,9)	linear portion of program; computes average detector voltage and extinction constant, and prints them, returns to label M

- * marks labels which are subroutines
- () hold subroutines and labels branched to

APPENDIX C

The following is a complete listing of the program as printed out by the calculator;

0000	GTO	44	0050	LBL	51	0100	+	33
0001	LBL	51	0051	DN	25	0101	DN	25
0002	L	72	0052	LBL	51	0102	CNT	47
0003	LBL	51	0053	UP	27	0103	S/R	77
0004	A	62	0054	FMT	42	0104	LBL	51
0005	IFG	43	0055	1	01	0105	B	66
0006	SFL	54	0056	8	10	0106	a	13
0007	GTO	44	0057	0	00	0107	UP	27
0008	LBL	51	0058	1	01	0108	IFG	43
0009	UP	27	0059	XTO	23	0109	SFL	54
0010	FMT	42	0060	+	33	0110	GTO	44
0011	1	01	0061	0	13	0111	LBL	51
0012	8	10	0062	0	13	0112	1	01
0013	3	03	0063	UP	27	0113	CNT	47
0014	FMT	42	0064	CLX	37	0114	1	01
0015	3	03	0065	STP	41	0115	9	11
0016	3	03	0066	XTO	23	0116	5	05
0017	.	21	0067	6	06	0117	GTO	44
0018	UP	27	0068	0	00	0118	LBL	51
0019	CLX	37	0069	FMT	42	0119	2	02
0020	X=Y	50	0070	1	01	0120	LBL	51
0021	GTO	44	0071	8	10	0121	1	01
0022	LBL	51	0072	3	03	0122	CNT	47
0023	A	62	0073	LBL	51	0123	1	01
0024	CNT	47	0074	DN	25	0124	2	02
0025	EEX	26	0075	XFR	67	0125	3	03
0026	CHS	32	0076	5	05	0126	LBL	51
0027	3	03	0077	4	04	0127	2	02
0028	X	36	0078	XTO	23	0128	S/R	77
0029	DN	25	0079	b	14	0129	LBL	51
0030	UP	27	0080	1/X	17	0130	C	61
0031	INT	64	0081	UP	27	0131	a	13
0032	-	34	0082	1	01	0132	UP	27
0033	XTO	23	0083	0	00	0133	IFG	43
0034	6	06	0084	DIV	35	0134	SFL	54
0035	0	00	0085	XFR	67	0135	FTO	44
0036	EEX	26	0086	6	06	0136	LBL	51
0037	3	03	0087	0	00	0137	3	03
0038	X	36	0088	X<Y	52	0138	1	01
0039	2	02	0089	CNT	47	0139	9	11
0040	0	00	0090	S/R	77	0140	9	11
0041	0	00	0091	CNT	47	0141	GTO	44
0042	X<Y	52	0092	CNT	47	0142	LBL	51
0043	CNT	47	0093	UP	27	0143	4	04
0044	-	34	0094	a	13	0144	LBL	51
0045	CNT	47	0095	UP	27	0145	3	03
0046	CNT	47	0096	EEX	26	0146	1	01
0047	YTO	40	0097	3	03	0147	2	02
0048	0	13	0098	DIV	35	0148	8	10
0049	GTO	44	0099	DN	25	0149	LBL	51

0150	4	04	0200	GTO	44	0250	4	04
0151	S/R	77	0201	LBL	51	0251	XFR	67
0152	LBL	51	0202	5	05	0252	X	36
0153	D	63	0203	CNT	47	0253	a	13
0154	FTO	44	0204	XFR	67	0254	XTO	23
0155	S/R	77	0205	6	06	0255	+	33
0156	LBL	51	0206	0	00	0256	5	05
0157	A	62	0207	I	65	0257	LBL	51
0158	XFR	67	0208	XFR	67	0258	5	05
0159	6	06	0209	X	36	0259	GTO	44
0160	0	00	0210	6	06	0260	S/R	77
0161	UP	27	0211	1	01	0261	LBL	51
0162	√	76	0212	XTO	23	0262	C	61
0163	XTO	23	0213	+	33	0263	X>Y	53
0164	6	06	0214	6	06	0264	GTO	44
0165	1	01	0215	XFR	67	0265	LBL	51
0166	b	14	0216	X	36	0266	D	63
0167	X	36	0217	a	13	0267	CNT	47
0168	a	13	0218	XTO	23	0268	S/R	77
0169	FMT	42	0219	+	33	0269	LBL	51
0170	1	01	0220	7	07	0270	E	60
0171	UP	27	0221	XFR	67	0271	a	13
0172	FMT	42	0222	X	36	0272	UP	27
0173	1	01	0223	a	13	0273	XSQ	12
0174	4	04	0224	XTO	23	0274	XFR	67
0175	CNT	47	0225	+	33	0275	X	36
0176	5	05	0226	8	10	0276	1	01
0177	UP	27	0227	XFR	67	0277	YE	24
0178	a	13	0228	6	06	0278	X	36
0179	X<Y	52	0229	1	01	0279	2	02
0180	GTO	44	0230	XTO	23	0280	XFR	67
0181	LBL	51	0231	+	33	0281	+	33
0182	5	05	0232	1	01	0282	3	03
0183	CNT	47	0233	XFR	67	0283	+	33
0184	GTO	44	0234	X	36	0284	DN	25
0185	S/R	77	0235	a	13	0285	J	75
0186	LBL	51	0236	XTO	23	0286	XFR	67
0187	B	66	0237	+	33	0287	X	36
0188	X<Y	52	0238	2	02	0288	b	14
0189	GTO	44	0239	XFR	67	0289	UP	27
0190	LBL	51	0240	X	36	0290	a	13
0191	5	05	0241	a	13	0291	FMT	42
0192	CNT	47	0242	XTO	23	0292	1	01
0193	XFR	67	0243	+	33	0293	DN	25
0194	6	06	0244	3	03	0294	1	01
0195	0	00	0245	XFR	67	0295	XTO	23
0196	UP	27	0246	X	36	0296	+	33
0197	b	14	0247	a	13	0297	a	13
0198	1/X	17	0248	XTO	23	0298	a	13
0199	X>Y	53	0249	+	3	0299	UP	27

0300	2	02	0350	-	34	0400	9	11
0301	0	00	0351	UP	27	0401	8	10
0302	0	00	0352	1	01	0402	XTO	23
0303	X<Y	53	0353	-	34	0403	1	01
0304	GTO	44	0354	RUP	22	0404	0	00
0305	LBL	51	0355	+	33	0405	4	04
0306	E	60	0356	DN	25	0406	XFR	67
0307	CNT	47	0357	K	55	0407	9	11
0308	XFR	67	0358	5	05	0408	5	05
0309	2	02	0359	FMT	42	0409	FMT	42
0310	1	01	0360	1	01	0410	1	01
0311	UP	27	0361	8	10	0411	PNT	45
0312	F	16	0362	3	03	0412	XFR	67
0313	XFR	67	0363	YTO	40	0314	9	11
0314	2	02	0364	5	05	0414	7	07
0315	2	02	0365	0	00	0415	XTO	23
0316	UP	27	0366	FMT	42	0416	+	33
0317	F	16	0367	1	01	0417	1	01
0318	XFR	67	0368	PNT	45	0418	0	00
0319	2	02	0369	FMT	42	0419	3	03
0320	3	03	0370	1	01	0420	1	01
0321	UP	27	0371	FMT	42	0421	XTO	23
0322	F	16	0372	CNT	47	0422	+	33
0323	S/R	77	0373	FMT	42	0423	9	11
0324	LBL	51	0374	FMT	42	0424	5	05
0325	F	16	0375	1	01	0425	GTO	44
0326	CLX	37	0376	8	10	0426	LBL	51
0327	XEY	30	0377	0	00	0427	H	74
0328	FMT	42	0378	XFR	67	0428	LBL	51
0329	1	01	0379	5	05	0429	6	06
0330	UP	27	0380	0	00	0430	CLR	20
0331	FMT	42	0381	FMT	42	0431	FMT	42
0332	DN	25	0382	1	01	0432	1	01
0333	UP	27	0383	PNT	45	0433	UP	27
0334	1	01	0384	S/R	77	0434	1	01
0335	5	05	0385	LBL	51	0435	9	11
0336	0	00	0386	H	74	0436	0	00
0337	0	00	0387	XFR	67	0437	XTO	23
0338	XEY	30	0388	1	01	0438	-	34
0339	FMT	42	0389	0	00	0439	1	01
0340	DN	25	0390	3	03	0440	0	00
0341	FMT	42	0391	UP	27	0441	3	03
0342	UP	27	0392	XFR	67	0442	XFR	67
0343	S/R	77	0393	9	11	0443	1	01
0344	LBL	51	0394	X<Y	52	0444	0	00
0345	G	15	0395	GTO	44	0445	4	04
0346	K	55	0396	LBL	51	0446	XTO	23
0347	4	04	0397	6	06	0447	0	00
0348	UP	27	0398	CNT	47	0448	9	11
0349	INT	64	0399	XFR	67	0449	8	10

0450	2	02	0500	XTO	23	0550	0	71
0451	0	00	0501	+	33	0551	A	62
0452	UP	27	0502	9	11	0552	D	63
0453	XFR	67	0503	5	05	0553	CNT	47
0454	9	11	0504	GTO	44	0554	D	63
0455	9	11	0505	LBL	51	0555	A	62
0456	DIV	35	0605	7	07	0556	XTO	23
0457	XFR	67	0507	S/R	77	0557	A	62
0458	9	11	0508	LBL	51	0558	FMT	42
0459	X	36	0509	I	65	0559	STP	41
0460	YTO	40	0510	XFR	67	0560	IFG	43
0461	9	11	0511	5	05	0561	CNT	47
0462	7	07	0512	7	07	0562	SFL	54
0463	CLX	37	0513	XFR	67	0563	S/R	77
0464	XTO	23	0514	DIV	35	0564	CNT	47
0465	9	11	0515	5	05	0565	FMT	42
0466	5	05	0516	5	05	0566	FMT	42
0467	LBL	51	0517	UP	27	0567	π	56
0468	7	07	0518	XFR	67	0568	I	65
0469	XFR	67	0519	3	03	0569	π	56
0470	9	11	0520	1	01	0570	CNT	47
0471	8	10	0521	XSQ	12	0571	O	71
0472	XTO	23	0522	X	36	0572	N	73
0473	1	01	0523	DN	25	0573	CNT	47
0474	0	00	0524	1/X	17	0574	π	56
0475	4	04	0525	XFR	67	0575	a	13
0476	UP	27	0526	X	36	0576	I	65
0477	XFR	67	0527	5	05	0577	N	73
0478	9	11	0528	6	06	0578	XTO	23
0479	X<Y	52	0529	1	65	0579	IFG	43
0480	CNT	47	0530	XFR	67	0580	FMT	42
0481	S/R	77	0531	DIV	35	0581	STP	41
0482	CNT	47	0532	3	03	0582	S/R	77
0483	CNT	47	0533	1	01	0583	LBL	51
0484	XFR	67	0534	XTO	23	0584	K	55
0485	9	11	0535	5	05	0585	FMT	42
0486	5	05	0536	8	10	0586	1	01
0487	FMT	42	0537	S/R	77	0587	8	10
0488	1	01	0538	LBL	51	0588	3	03
0489	PNT	45	0539	J	75	0589	FMT	42
0490	XFR	67	0540	FMT	42	0590	3	03
0491	9	11	0541	FMT	42	0591	3	03
0492	7	07	0542	F	16	0592	.	21
0493	XTO	23	0543	L	72	0593	UP	27
0494	+	33	0544	A	62	0594	EEX	26
0495	0	00	0545	G	15	0595	3	03
0496	9	11	0546	CNT	47	0596	DIV	35
0497	8	10	0547	EEX	26	0597	UP	27
0498	2	02	0548	CNT	47	0598	DN	25
0499	0	00	0549	L	72	0599	X<Y	52

0600	DN	25	0650	D	63	0700	S/R	77
0601	PNT	45	0651	A	62	0701	LBL	51
0602	CNT	47	0652	XFR	67	0702	K	55
0603	CNT	47	0653	IFG	43	0703	FMT	42
0604	DN	25	0654	FMT	42	0704	1	01
0605	INT	64	0655	XFR	67	0705	8	10
0606	-	34	0656	5	05	0706	1	01
0607	.	21	0657	2	02	0707	FMT	42
0608	2	02	0658	STP	41	0708	FMT	42
0609	X<Y	52	0659	XTO	23	0709	1	01
0610	-	34	0660	5	05	0710	YTO	40
0611	CNT	47	0661	2	02	0711	XTO	23
0612	CNT	47	0662	PNT	45	0712	CNT	47
0613	CNT	47	0663	FMT	42	0713	C	61
0614	.	21	0664	FMT	42	0714	A	62
0615	1	01	0665	XFR	67	0715	L	72
0616	9	11	0666	E	60	0716	IFG	43
0617	9	11	0667	A	62	0717	FMT	42
0618	X<Y	53	0668	a	13	0718	XFR	67
0619	GTO	44	0669	IFG	43	0719	2	02
0620	LBL	51	0670	FMT	42	0720	1	01
0621	K	55	0671	XFR	67	0721	STP	41
0622	CNT	47	0672	5	05	0722	XTO	23
0623	S/R	77	0673	3	03	0723	2	02
0624	LBL	51	0674	STP	41	0724	1	01
0625	L	72	0675	XTO	23	0725	PNT	45
0626	FMT	42	0676	5	05	0726	FMT	42
0627	1	01	0677	3	03	0727	FMT	42
0628	8	10	0678	PNT	45	0728	2	02
0629	0	00	0679	CLX	37	0729	N	73
0630	CLR	20	0680	FMT	42	0730	D	63
0631	FMT	42	0681	FMT	42	0731	CNT	47
0632	FMT	42	0682	F	16	0732	C	61
0633	M	70	0683	L	72	0733	A	62
0634	O	71	0684	A	62	0734	L	72
0635	N	73	0685	G	15	0735	IFG	43
0636	XTO	23	0686	CNT	47	0736	FMT	42
0637	H	74	0687	EEX	26	0737	XFR	67
0638	IFG	43	0688	CNT	47	0738	2	02
0639	FMT	42	0689	C	61	0739	2	02
0640	XFR	67	0690	A	62	0740	STP	41
0641	5	05	0691	L	72	0741	XTO	23
0642	1	01	0692	CNT	47	0742	2	02
0643	STP	41	0693	π	56	0743	2	02
0644	XTO	23	0694	XTO	23	0744	PNT	45
0645	5	05	0695	YTO	40	0745	FMT	42
0646	1	01	0696	FMT	42	0746	FMT	42
0647	PNT	45	0697	STP	41	0747	3	03
0648	FMT	42	0698	IFG	43	0748	a	13
0649	FMT	42	0699	GTO	44	0749	D	63

0750	CNT	47	0800	7	07	0850	PNT	45
0751	C	61	0801	9	11	0851	LBL	51
0752	A	62	0802	PNT	45	0852	M	70
0753	L	72	0803	XFR	67	0853	CLR	20
0754	IFG	43	0804	7	07	0854	FMT	42
0755	FMT	42	0805	8	10	0855	FMT	42
0756	XFR	67	0806	UP	27	0856	IND	31
0757	2	02	0807	XFR	67	0857	A	62
0758	3	03	0808	7	07	0858	INT	64
0759	STP	41	0809	9	11	0859	E	60
0760	XTO	23	0810	I	65	0860	L	72
0761	2	02	0811	XEY	30	0861	E	60
0762	3	03	0812	I	65	0862	N	73
0763	PNT	45	0813	-	34	0863	G	15
0764	FMT	42	0814	XFR	67	0864	XTO	23
0765	FMT	42	0815	2	02	0865	H	74
0766	INT	64	0816	3	03	0866	CLR	20
0767	1	01	0817	XFR	67	0867	X<Y	52
0768	EEX	26	0818	-	34	0868	M	70.
0769	XFR	67	0819	2	02	0869	I	65
0770	CNT	47	0820	1	01	0870	C	61
0771	A	62	0821	DIV	35	0871	a	13
0772	N	73	0822	YTO	40	0872	0	71
0773	D	63	0823	6	06	0873	N	73
0774	CNT	47	0824	5	05	0874	YTO	40
0775	INT	64	0825	CLR	20	0875	PSE	57
0776	3	03	0826	FMT	42	0876	IFG	43
0777	EEX	26	0827	FMT	42	0877	FMT	42
0778	YE	24	0828	E	60	0878	FMT	42
0779	FMT	42	0829	YE	24	0879	1	01
0780	FMT	42	0830	XTO	23	0880	8	10
0781	1	01	0831	1	65	0881	4	04
0782	8	10	0832	N	73	0882	XFR	67
0783	2	02	0833	C	61	0883	4	04
0784	YE	24	0834	XTO	23	0884	1	01
0785	7	07	0835	CNT	47	0885	STP	41
0786	8	10	0836	C	61	0886	XTO	23
0787	XFR	67	0837	0	71	0887	4	04
0788	7	07	0838	N	73	0888	1	01
0789	9	11	0839	YTO	40	0869	PNT	45
0790	STP	41	0840	XTO	23	0890	UP	27
0791	YTO	40	0841	IFG	43	0891	EEX	26
0792	7	07	0842	FMT	42	0892	6	06
0793	8	10	0843	XFR	67	0893	DIV	35
0794	XTO	23	0844	5	05	0894	YTO	40
0795	7	07	0845	6	06	0895	3	03
0796	9	11	0846	STP	41	0896	0	00
0797	XEY	30	0847	XTO	23	0897	CLR	20
0798	PNT	45	0848	5	05	0898	FMT	42
0799	XFR	67	0849	6	06	0899	FMT	42

0900	a	13	0950	C	61	1000	N	73
0901	A	62	0951	0	71	1001	E	60
0902	N	73	0952	1/X	17	1002	A	62
0903	G	15	0953	N	73	1003	a	13
0904	E	60	0954	XTO	23	1004	FMT	42
0905	CNT	47	0955	IFG	43	1005	STP	41
0906	X<Y	52	0956	FMT	42	1006	IFG	43
0907	M	70	0957	CLR	20	1007	GTO	44
0908	E	60	0958	5	05	1008	LBL	51
0909	XTO	23	0959	EEX	26	1009	N	73
0910	E	60	0960	3	03	1010	CNT	47
0911	a	13	0961	STP	41	1011	CLR	20
0912	YTO	40	0962	UP	27	1012	FMT	42
0918	PSE	57	0963	PNT	45	1013	1	01
0914	IFG	43	0964	DN	25	1014	UP	27
0915	FMT	42	0965	1/X	17	1015	2	02
0916	FMT	42	0966	UP	27	1016	0	00
0917	1	01	0967	5	05	1017	FMT	42
0918	8	10	0968	X	36	1018	1	01
0919	0	00	0969	YTO	40	1019	5	05
0920	XFR	67	0970	5	05	1020	1	01
0921	3	03	0971	4	04	1021	FMT	42
0922	1	01	0972	CLR	20	1022	1	01
0923	STP	41	0973	FMT	42	1023	6	06
0924	XTO	23	0974	FMT	42	1024	4	04
0925	3	03	0975	XTO	23	1025	0	00
0926	1	01	0976	I	65	1026	0	00
0927	PNT	45	0977	M	70	1027	XTO	23
0928	FMT	42	0978	E	60	1028	0	00
0929	FMT	42	0979	IFG	43	1029	9	11
0930	G	15	0980	FMT	42	1030	8	10
0931	A	62	0981	XFR	67	1031	XFR	67
0932	I	65	0982	2	02	1032	9	11
0933	N	73	0983	8	10	1033	XFR	67
0934	IFG	43	0984	STP	41	1034	DIV	35
0935	FMT	42	0985	XTO	23	1035	1	01
0936	XFR	67	0986	2	02	1036	0	00
0937	5	05	0987	8	10	1037	0	00
0938	5	05	0988	PNT	45	1038	XTO	23
0939	STP	41	0989	FMT	42	1039	9	11
0940	XTO	23	0990	FMT	42	1040	7	07
0941	5	05	0991	F	16	1041	FMT	42
0942	5	05	0992	L	72	1042	1	01
0943	PNT	45	0993	A	62	1043	8	10
0944	FMT	42	0994	G	15	1044	0	00
0945	FMT	42	0995	CNT	47	1045	CLX	37
0946	M	70	0996	EEX	26	1046	XTO	23
0947	A	62	0997	CNT	47	1047	9	11
0948	YE	24	0998	L	72	1048	5	05
0949	CNT	47	0999	I	65	1049	GTO	44

1050	S/R	77	1100	+	33	1150	X	36
1051	LBL	51	1101	+	33	1151	7	07
1052	H	74	1102	XFR	67	1152	+	33
1053	CLR	20	1103	3	03	1153	XFR	67
1054	XTO	23	1104	XSQ	12	1154	3	03
1055	1	01	1105	XFR	67	1155	XSQ	12
1056	XTO	23	1106	X	36	1156	XFR	67
1057	2	02	1107	3	03	1157	X	36
1058	XTO	23	1108	-	34	1158	6	06
1059	3	03	1109	XFR	67	1159	-	34
1060	XTO	23	1110	2	02	1160	XFR	67
1061	4	04	1111	XSQ	12	1161	2	02
1062	XTO	23	1112	XFR	67	1162	XSQ	12
1063	5	05	1113	X	36	1163	XFR	67
1064	XTO	23	1114	5	05	1164	X	36
1065	6	06	1115	-	34	1165	8	10
1066	XTO	23	1116	XFR	67	1166	-	34
1067	7	07	1117	4	04	1167	XFR	67
1068	XTO	23	1118	XSQ	12	1168	1	01
1069	8	10	1119	XFR	67	1169	XFR	67
1070	CNT	47	1120	X	36	1170	X	36
1071	GTO	44	1121	1	01	1171	4	04
1072	S/R	77	1122	-	34	1172	XFR	67
1073	LBL	51	1123	YTO	40	1173	X	36
1074	J	75	1124	1	01	1174	7	07
1075	GTO	44	1125	0	00	1175	-	34
1076	S/R	77	1126	XFR	67	1176	YTO	40
1077	LBL	51	1127	8	10	1177	1	01
1078	D	63	1128	XFR	67	1178	1	01
1079	FMT	42	1129	X	36	1179	XFR	67
1080	1	01	1130	3	03	1180	1	01
1081	8	10	1131	XFR	67	1181	XFR	67
1082	0	00	1132	X	36	1182	X	36
1083	XFR	67	1133	1	01	1183	5	05
1084	5	05	1134	UP	27	1184	XFR	67
1085	XFR	67	1135	XFR	67	1185	X	36
1086	X	36	1136	4	04	1186	7	07
1087	3	03	1137	XFR	67	1187	UP	27
1088	XFR	67	1138	X	36	1188	XFR	67
1089	X	36	1139	2	02	1189	8	10
1090	1	01	1140	XFR	67	1190	XFR	67
1091	UP	27	1141	X	36	1191	X	36
1092	XFR	67	1142	6	06	1192	2	02
1093	4	04	1143	+	33	1193	XFR	67
1094	XFR	67	1144	XFR	67	1194	X	36
1095	X	36	1145	2	02	1195	3	03
1096	2	02	1146	XFR	67	1196	+	33
1097	XFR	67	1147	X	36	1197	XFR	67
1098	X	36	1148	3	03	1198	3	03
1099	3	03	1149	XFR	67	1199	XFR	67

1200	X	36	1250	7	07	1300	DIV	35
1201	4	04	1251	+	33	1301	1	01
1202	XFR	67	1252	XFR	67	1302	0	00
1203	X	36	1253	2	02	1303	XTO	23
1204	6	06	1254	XFR	67	1304	2	02
1205	+	33	1255	X	36	1305	XFR	67
1206	XFR	67	1256	4	04	1306	1	01
1207	3	03	1257	XFR	67	1307	3	03
1208	XSQ	12	1258	X	36	1308	XFR	67
1209	XFR	67	1259	8	10	1309	DIV	35
1210	X	36	1260	+	33	1310	1	01
1211	7	07	1261	XFR	67	1311	0	00
1212	-	34	1262	3	03	1312	XTO	23
1213	XFR	67	1263	XSQ	12	1313	3	03
1214	2	02	1264	XFR	67	1314	.	21
1215	XFR	67	1265	X	36	1315	5	05
1216	X	36	1266	8	10	1316	XFR	67
1217	5	05	1267	-	34	1317	DIV	35
1218	XFR	67	1268	XFR	67	1318	1	01
1219	X	36	1269	2	02	1319	CHS	32
1220	6	06	1270	XFR	67	1320	UP	27
1221	-	34	1271	X	36	1321	XFR	67
1222	XFR	67	1272	5	05	1322	6	06
1223	1	01	1273	XFR	67	1323	5	05
1224	XFR	67	1274	X	36	1324	XSQ	12
1225	X	36	1275	7	07	1325	X	36
1226	4	04	1276	-	34	1326	YTO	40
1227	XFR	67	1277	XFR	67	1327	2	02
1228	X	36	1278	4	04	1328	5	05
1229	8	10	1279	XSQ	12	1329	DN	25
1230	√	34	1280	XFR	67	1330	-	76
1231	YTO	40	1281	X	36	1331	XTO	23
1232	1	01	1282	6	06	1332	1	01
1233	2	02	1283	-	34	1333	4	04
1234	XFR	67	1284	YTO	40	1334	CNT	47
1235	3	03	1285	1	01	1335	1	01
1236	XFR	67	1286	3	03	1336	0	00
1237	X	36	1287	XFR	67	1337	.	21
1238	5	05	1288	1	01	1338	2	02
1239	XFR	67	1289	1	01	1339	UP	27
1240	X	36	1290	XFR	67	1340	5	05
1241	6	06	1291	DIV	35	1341	FMT	42
1242	UP	27	1292	1	01	1342	1	01
1243	XFR	67	1293	0	00	1343	UP	27
1244	3	03	1294	XTO	23	1344	FMT	42
1245	XFR	67	1295	1	01	1345	1	01
1246	X	36	1296	XFR	67	1346	FMT	42
1247	4	04	1297	1	01	1347	D	63
1248	XFR	67	1298	2	02	1348	A	62
1249	X	36	1299	XFR	67	1349	XTO	23

1350	E	60	1400	.	21	1450	1	01
1351	CNT	47	1401	9	11	1451	PNT	45
1352	FMT	42	1402	UP	27	1452	9	11
1353	XFR	67	1403	5	05	1453	.	21
1354	5	05	1404	FMT	42	1454	6	06
1355	1	01	1405	1	01	1455	UP	27
1356	FMT	42	1406	UP	27	1456	5	05
1357	1	01	1407	FMT	42	1457	FMT	42
1358	PNT	45	1408	1	01	1458	1	01
1359	FMT	42	1409	FMT	42	1459	UP	27
1360	1	01	1410	L	72	1460	FMT	42
1361	FMT	42	1411	M	70	1461	1	01
1362	DIV	35	1412	B	66	1462	FMT	42
1363	FMT	42	1413	D	63	1463	LBL	51
1364	XFR	67	1414	CNT	47	1464	CNT	47
1365	5	05	1415	SFL	54	1465	YTO	40
1366	2	02	1416	CNT	47	1466	b	14
1367	FMT	42	1417	FMT	42	1467	CNT	47
1368	1	01	1418	FMT	42	1468	SFL	54
1369	PNT	45	1419	1	01	1469	CNT	47
1370	FMT	42	1420	8	10	1470	FMT	42
1371	1	01	1421	4	04	1471	FMT	42
1372	FMT	42	1422	XFR	67	1472	1	01
1373	DIV	35	1423	4	04	1473	8	10
1374	FMT	42	1424	1	01	1474	3	03
1375	XFR	67	1425	FMT	42	1475	XFR	67
1376	5	05	1426	1	01	1476	2	02
1377	3	03	1427	PNT	45	1477	5	05
1378	FMT	42	1428	FMT	42	1478	FMT	42
1379	1	01	1429	1	01	1479	1	01
1380	PNT	45	1430	8	10	1480	PNT	45
1381	FMT	42	1431	0	00	1481	FMT	42
1382	1	01	1432	FMT	42	1482	1	01
1383	FMT	42	1433	1	01	1483	FMT	42
1384	CNT	47	1434	FMT	42	1484	CNT	47
1385	CNT	47	1435	CNT	47	1485	CNT	47
1386	CNT	47	1436	CNT	47	1486	CNT	47
1387	XTO	23	1437	CNT	47	1487	LBL	51
1388	I	65	1438	a	13	1488	CNT	47
1389	M	70	1439	N	73	1489	SFL	54
1390	E	60	1440	G	15	1490	CNT	47
1391	CNT	47	1441	E	60	1491	FMT	42
1392	FMT	42	1442	CNT	47	1492	XFR	67
1393	XFR	67	1443	SFL	54	1493	1	01
1394	2	02	1444	CNT	47	1494	4	04
1395	8	10	1445	FMT	42	1495	FMT	42
1396	FMT	42	1446	XFR	67	1496	1	01
1397	1	01	1447	3	03	1497	PNT	45
1398	PNT	45	1448	1	01	1498	XFR	67
1399	9	11	1449	FMT	42	1499	3	03

1500	0	00	1550	FMT	42	1600	CNT	47
1501	UP	27	1551	1	01	1601	INT	64
1502	2	02	1552	FMT	42	1602	CNT	47
1503	DIV	35	1553	C	61	1603	SFL	54
1504	π	56	1554	N	73	1604	CNT	47
1505	DIV	35	1555	YTO	40	1605	FMT	42
1506	7	07	1556	b	14	1606	FMT	42
1507	UP	27	1557	CNT	47	1607	1	01
1508	6	06	1558	SFL	54	1608	8	10
1509	DIV	35	1559	CNT	47	1609	3	03
1510	DN	25	1560	FMT	42	1610	XFR	67
1511	XEY	30	1561	XFR	67	1611	1	01
1512	H	74	1562	2	02	1612	CHS	32
1513	XTO	23	1563	5	05	1613	1/X	17
1514	X	36	1564	GTO	44	1614	XFR	67
1515	2	02	1565	S/R	77	1615	X	36
1516	5	05	1566	LBL	51	1616	2	02
1517	XFR	67	1567	G	15	1617	UP	27
1518	3	03	1568	FMT	42	1618	2	02
1519	1	01	1569	1	01	1619	DIV	35
1520	UP	27	1570	FMT	42	1620	XFR	67
1521	1	01	1571	CNT	47	1621	2	02
1522	1	01	1572	CNT	47	1622	3	03
1523	UP	27	1573	CNT	47	1623	-	34
1524	6	06	1574	C	61	1624	XFR	67
1525	DIV	35	1575	N	73	1625	6	06
1526	DN	25	1576	CNT	47	1626	5	05
1527	XEY	30	1577	SFL	54	1627	X	36
1528	H	74	1578	CNT	47	1628	XFR	67
1529	XTO	23	1579	FMT	42	1629	7	07
1530	DIV	35	1580	XFR	67	1630	9	11
1531	2	02	1581	2	02	1631	I	65
1532	5	05	1582	5	05	1632	+	33
1533	.	21	1583	$\sqrt{\quad}$	76	1633	XFR	67
1534	4	04	1584	GTO	44	1634	1	01
1535	9	11	1585	S/R	77	1635	4	04
1536	6	06	1586	LBL	51	1636	XSQ	12
1537	XTO	23	1587	G	15	1637	UP	27
1538	DIV	35	1588	9	11	1638	2	02
1539	2	02	1589	UP	27	1639	DIV	35
1540	5	05	1590	5	05	1640	DN	25
1541	CNT	47	1591	FMT	42	1641	+	33
1542	9	11	1592	1	01	1642	DN	25
1543	.	21	1593	UP	27	1643	J	75
1544	3	03	1594	FMT	42	1644	XTO	23
1545	UP	27	1595	1	01	1645	5	05
1546	5	05	1596	FMT	42	1646	7	07
1547	FMT	42	1597	A	62	1647	FMT	42
1548	1	01	1598	INT	64	1648	1	01
1549	UP	27	1599	E	60	1649	PNT	45

1650	GTO	44	1700	XTO	23	1750	S/R	77
1651	S/R	77	1701	a	13	1751	LBL	51
1652	LBL	51	1702	FMT	42	1752	B	66
1653	I	65	1703	1	01	1753	XEY	30
1654	FMT	42	1704	UP	27	1754	X>Y	53
1655	1	01	1705	GTO	44	1755	GTO	44
1656	FMT	42	1706	S/R	77	1756	LBL	51
1657	CNT	47	1707	LBL	51	1757	9	11
1658	CNT	47	1708	E	60	1758	CNT	47
1659	CNT	47	1709	1	01	1759	XEY	30
1660	M	70	1710	0	00	1760	5	05
1661	1/X	17	1711	.	21	1761	X>Y	53
1662	CNT	47	1712	5	05	1762	GTO	44
1663	SFL	54	1713	UP	27	1763	LBL	51
1664	CNT	47	1714	5	05	1764	8	10
1665	FMT	42	1715	FMT	42	1765	CNT	47
1666	XFR	67	1716	1	01	1766	XFR	67
1667	5	05	1717	UP	27	1767	6	06
1668	8	10	1718	FMT	42	1768	0	00
1669	GTO	44	1719	FMT	42	1769	X	36
1670	S/R	77	1720	E	60	1770	YTO	40
1671	LBL	51	1721	N	73	1771	+	33
1672	G	15	1722	D	63	1772	6	06
1673	8	10	1723	CLR	20	1773	9	11
1674	.	21	1724	CLR	20	1774	XTO	23
1675	7	07	1725	FMT	42	1775	+	33
1676	UP	27	1726	STP	41	1776	6	06
1677	5	05	1727	GTO	44	1777	8	10
1678	FMT	42	1728	LBL	51	1778	GTO	44
1679	1	01	1729	M	70	1779	LBL	51
1680	UP	27	1730	LBL	51	1780	8	10
1681	FMT	42	1731	N	73	1781	LBL	51
1682	1	01	1732	CLX	37	1782	9	11
1683	FMT	42	1733	XTO	23	1783	FMT	42
1684	G	15	1734	6	06	1784	FMT	42
1685	A	62	1735	9	11	1785	A	62
1686	I	65	1736	XTO	23	1786	INT	64
1687	N	73	1737	6	06	1787	E	60
1688	CNT	47	1738	8	10	1788	CNT	47
1689	SFL	54	1739	GTO	44	1789	INT	64
1690	CNT	47	1740	S/R	77	1790	CNT	47
1691	FMT	42	1741	LBL	51	1791	SFL	54
1692	XFR	67	1742	J	75	1792	CNT	47
1693	5	05	1743	LBL	51	1793	FMT	42
1694	5	05	1744	8	10	1794	XFR	67
1695	FMT	42	1745	GTO	44	1795	6	06
1696	1	01	1746	S/R	77	1796	9	11
1697	PNT	45	1747	LBL	51	1797	XFR	67
1698	CLX	37	1748	A	62	1798	DIV	35
1699	UP	27	1749	GTO	44	1799	6	06

1800	8	10	1850	8	10
1801	UP	27	1851	PNT	45
1802	XFR	67	1852	FMT	42
1803	2	02	1853	FMT	42
1804	3	03	1854	E	60
1805	-	34	1855	N	73
1806	XFR	67	1856	D	63
1807	-	34	1857	CLR	20
1808	2	02	1858	CLR	20
1809	1	01	1859	FMT	42
1810	DIV	35	1860	STP	41
1811	XFR	67	1861	GTO	44
1812	7	07	1862	LBL	51
1813	9	11	1863	M	70
1814	XFR	67	1864	END	46
1815	-	34			
1816	7	07			
1817	8	10			
1818	X	36			
1819	XFR	67			
1820	7	07			
1821	9	11			
1822	+	33			
1823	DN	25			
1824	XTO	23			
1825	5	05			
1826	7	07			
1827	FMT	42			
1828	1	01			
1829	7	07			
1830	PNT	45			
1831	PNT	45			
1832	GTO	44			
1833	S/R	77			
1834	LBL	51			
1835	I	65			
1836	FMT	42			
1837	FMT	42			
1938	E	60			
1839	YE	24			
1840	XTO	23			
1841	CNT	47			
1842	M	70			
1843	1/X	17			
1844	CNT	47			
1845	SFL	54			
1846	CNT	47			
1847	FMT	42			
1848	XFR	67			
1849	5	05			

BIBLIOGRAPHY

1. Tatarski, U. I., Wave Propagation In A Turbulent Medium, McGraw-Hill, 1961.
2. Strohbehn, J. W., "Line-of-sight Wave Propagation Through The Turbulent Atmosphere", Proceedings of the IEEE, Vol. 56, pp. 1301-1317, August 1968.
3. Haagensen, B. C., Laser Beam Scintillation in the Marine Boundary Layer, M.S. Thesis, United States Naval Postgraduate School, Monterey, California, 1973.
4. Schroeder, A. F., Laser Scintillation Properties in the Marine Boundary Layer, M.S. Thesis, United States Naval Postgraduate School, Monterey, California, 1973.
5. Cole, O. C. III, Shipboard Measurements of Laser Beam Scintillation in the Marine Boundary Layer, M.S. Thesis, United States Naval Postgraduate School, Monterey, California, 1974.
6. Anton, H., Elementary Linear Algebra, John Wiley & Sons, 1973.
7. Parrat, L. G., Probability and Experimental Errors In Science, Dover Publications, 1961.
8. Milne, W. E., Numerical Calculus, Princeton University Press, 1949.
9. Fishman, G. S., Concepts And Methods In Discrete Event Digital Simulation, Wylie Press, 1973.
10. Parrish, P. W., Shipboard Measurement of 0.6328 Micrometer Laser Beam Extinction In The Marine Boundary Layer, M.S. Thesis, United States Naval Postgraduate School, Monterey, California, 1976.
11. Hall, H. R., Aperture Averaging Effects on Scintillation and the Temporal Frequency Power Spectrum, M.S. Thesis, United States Naval Postgraduate School, Monterey, California, 1976.
12. Schwartz, H. W., An Experiment to Measure Broadband Beam Wander and Beam Spread in the Marine Boundary Layer, M.S. Thesis, United States Naval Postgraduate School, Monterey, California, 1976.

13. Signetics Corporation, Data Book, 1974.
14. Victoreen Instrument Company, Portable Instrument Package, PIP-400, Pulse Height Analyzer, 1967.
15. Hewlett-Packard Company, Hewlett-Packard 9810A Calculator Operating and Programming, 1971.
16. Hewlett-Packard Company, Hewlett-Packard 9810A Calculator Mathematics Block Operating Manual, 1971.
17. Hewlett-Packard Company, Hewlett-Packard 9810A Calculator Plotter Control Block Operating Manual, 1971.

INITIAL DISTRIBUTION LIST

	No. Copies
1. Defense Documentation Center Cameron Station Alexandria, Virginia 22314	2
2. Library, Code 0212 Naval Postgraduate School Monterey, California 93940	2
3. Professor K.E. Woehler, Code 61Wh Department of Physics and Chemistry Naval Postgraduate School Monterey, California 93940	2
4. Assoc. Professor E.A. Milne, Code 61Mn Department of Physics and Chemistry Naval Postgraduate School Monterey, California 93940	5
5. Lt. John R. Plett Class 53 SWOSCOLCOM, Bldg. 446 Newport, Rhode Island 02840	1

28 MAR 78

24026

Thesis

P6145 Plett

166483

c.1

Pulse height analyzer
interfacing and comput-
er programming in the
environmental laser
propagation project.

28 MAR 78

24026

Thesis

P6145

Plett

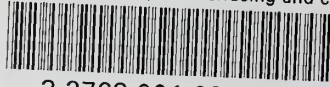
166483

c.1

Pulse height analyzer
interfacing and comput-
er programming in the
environmental laser
propagation project.

thesP6145

Pulse height analyzer interfacing and co



3 2768 001 92449 1

DUDLEY KNOX LIBRARY